Spatial variations in geochemical characteristics of the modern Mackenzie Delta sedimentary system

Jorien E. Vonk[1,2,*], Liviu Giosan[3], Jerzy Blusztajn[3], Daniel Montlucon[2], Elisabeth Graf Pannatier[4], Cameron McIntyre[5], Lukas Wacker[5], Robie W. Macdonald[6], Mark B. Yunker[7] and Timothy I. Eglinton[2]

(1) Utrecht University, Department of Earth Sciences, Utrecht and University of Groningen, Arctic Center, Groningen, The Netherlands
(2) Geological Institute, Swiss Federal Institute of Technology, Zürich, Switzerland
(3) Woods Hole Oceanographic Institution, Geology and Geophysics, Woods Hole, United States
(4) Swiss Federal Institute of Forest, Snow and Landscape Research, Birmensdorf, Switzerland
(5) Laboratory for Ion Beam Physics, Swiss Federal Institute of Technology, Zürich, Switzerland
(6) Institute of Ocean Sciences, Department of Fisheries and Oceans, Sidney, Canada
(7) 7137 Wallace Dr., Brentwood Bay, Canada
* Corresponding author: j.e.vonk@uu.nl, +31302535232, Utrecht University, Department of Earth Sciences, Budapestlaan 4, 3584 CD, Utrecht, The Netherlands

ABSTRACT

The Mackenzie River in Canada is by far the largest riverine source of sediment and organic carbon (OC) to the Arctic Ocean. Therefore the transport, degradation and burial of OC along the land-to-ocean continuum for this riverine system is important to study both regionally and as a dominant representative of Arctic rivers. Here, we apply sedimentological (grain size, mineral surface area), and organic and inorganic geochemical techniques (%OC, δ^{13}C-OC and Δ^{14}C-OC, ^{143}Nd/^{144}Nd, δ^{2}H and δ^{18}O, major and trace elements) on particulate, bank, channel and lake surface sediments from the Mackenzie Delta, as well as on surface sediments from the Mackenzie shelf in the Beaufort Sea. Our data show a hydrodynamic sorting effect resulting in the accumulation of finer-grained sediments in lake and shelf deposits. A general decrease in organic carbon (OC) to mineral surface area ratios from river-to-sea furthermore suggests a loss of mineral-bound terrestrial OC during transport through the delta and deposition on the shelf. The net isotopic value of the terrestrial OC that is lost en route, derived from relationships between δ^{13}C, OC and surface area, is -28.5‰ for δ^{13}C

and -417‰ for $\Delta^{14}C$. We calculated that OC burial efficiencies are around 55%, which are higher (~20%) than other large river systems such as the Amazon. Old sedimentary OC ages, up to 12 ^{14}C-ky, suggest the delivery of both a petrogenic OC source (with an estimated contribution of 19±9%) as well as a pre-aged terrestrial OC source. We calculated the ^{14}C-age of this pre-aged, biogenic, component to be about 6100 yrs, or -501‰, which illustrates that terrestrial OC in the watershed can reside for millennia in soils before being released into the river. Surface sediments in lakes across the delta (n=20) showed large variability in %OC (0.92% to 5.7%) and $\delta^{13}C$ (-30.7‰ to -23.5‰). High-closure lakes, flooding only at exceptionally high water levels, hold high sedimentary OC contents (> 2.5%) and young biogenic OC with a terrestrial or an autochthonous source whereas no-closure lakes, permanently connected to a river channel, hold sediments with pre-aged, terrestrial OC. The intermediate low-closure lakes, flooding every year during peak discharge, display the largest variability in OC content, age and source, likely reflecting variability in for example the length of river-lake connections, the distance to sediment source and the number of intermediate settling basins. Bank, channel and suspended sediment show variable $^{143}Nd/^{144}Nd$ values, yet there is a gradual but distinct spatial transition in $^{143}Nd/^{144}Nd$ (nearly three ε units; from -11.4 to -13.9) in the detrital fraction of lake surface sediments from the western to the eastern delta. This reflects the input of younger Peel River catchment material in the west and input of older geological source material in the east, and suggests that lake sediments can be used to assess variability in source watershed patterns across the delta.

1. INTRODUCTION

Fluvial transport of continental sediments to the oceans forms a key component of land-ocean interactions and is a reflection of large-scale watershed dynamics. The relatively small, nearly land-locked Arctic Ocean receives a disproportionately large amount of fluvial sediments from some of the largest rivers on Earth (Gordeev et al., 2006). The Mackenzie River is the single largest source of fluvial sediments to the Arctic Ocean (Holmes et al., 2002). While increases in freshwater transport from Eurasian Arctic Rivers have been demonstrated, North American Rivers do not show such a distinct trend

(Peterson et al., 2002; McClelland et al., 2006). The Mackenzie drainage basin, however, experiences one of the largest recent temperature increases in Canada (Cohen et al., 1997) with an average warming of about 1.5°C between 1950-1998 (Zhang et al., 2000), which impacts hydrology and permafrost (Smith et al., 2005; Déry et al., 2009; Lesack et al., 2014). This rapid increase can be expected to have important implications for growing season lengthening, vegetation changes and permafrost thaw. In particular, the active layer of permafrost in the watershed has deepened by 0.47 cm/yr between 1980 and 2002 (Oelke et al., 2004). As permafrost thaw is mostly manifested in increases in the flux and age of particulate organic carbon (Guo et al., 2007) instead of changes in the dissolved organic carbon load, the Mackenzie River catchment is a key region of expected future change.

The Mackenzie delta, stretching out over ca. 13,000 km^2, serves as a transition zone between the river and the ocean and represents a major area for sediment and organic carbon (OC) burial, receiving ca. 128 Mt of fluvial material per year (Carson et al., 1998). In addition to fluvial sediments, additional minor sediment sources can consist of autochthonous production in delta lakes (Tank et al., 2011) and marine material that is deposited in outer delta channels and lakes during common reverse flow events (Jenner and Hill, 1991). Previous work on the Mackenzie shelf shows that a major fraction of the particulate organic matter transported by the Mackenzie River and sediments in the Beaufort Sea is derived from ancient, petrogenic OC whereas modern OC is mostly vascular plant material in origin (Yunker et al., 2002; Goñi et al., 2005; Drenzek et al., 2007). During the annual spring freshet the entire delta is flooded, distributing about 25 km^3 of turbid water over the delta (Emmerton et al., 2007).

Deltas and estuaries of large rivers cover a relatively small area on Earth yet form an essential interface between terrestrial and oceanic carbon reservoirs (Bianchi and Allison, 2009). They serve both as a source and sink of carbon through increased remineralization and sedimentation processes, respectively. Globally, it is estimated that ~47 Mt of terrestrial OC is buried every year in deltaic sediments (Burdige, 2005). Estimates for OC burial in the Mackenzie delta vary; Macdonald et al. (1998) estimated that about 50% of the annual OC

delivery by the Mackenzie River (2.1 Mt) is trapped in the delta, while Goñi et al. (2005) stated that OC burial in the delta is likely only a minor process.

Previous studies have had too few samples to delineate the spatial patterns of sediment delivery across the delta, and consequently our understanding of the sediment provenance is still limited. In this paper, we identify spatial variations in sediment sources and sedimentation patterns in the Mackenzie delta and Mackenzie's inner shelf. We apply a range of different organic and inorganic geochemical techniques (%OC, δ^{13}C-OC and Δ^{14}C-OC, ^{143}Nd/^{144}Nd on the detrital fraction, δ^{2}H and δ^{18}O on river water, major and trace elements) and sedimentological techniques (grain size, mineral surface area) to gain insights into organic matter age and provenance, sedimentation and sorting processes in the delta, particle carbon loading and burial efficiency. To assess patterns across the entire delta, we analyze suspended particulate matter and bank sediments of the incoming major rivers (Mackenzie, Arctic Red, and Peel Rivers), in addition to mid-delta bank sediments (Middle Channel, East Channel), lake sediments in the upper, middle, lower and outer delta, channel sediments in the outer delta, and Mackenzie shelf sediments.

Information gained on this deltaic system is designed to serve as a framework for assessing the relationship between drainage basin properties and deltaic sedimentation. We seek to build a foundation for assessing how the Mackenzie delta will respond to future change, as well as whether sedimentary deposits within the delta can provide a history of past watershed dynamics.

2. SAMPLING AND METHODOLOGY

2.1 Study area

The Mackenzie River drains a watershed of 1.78x10^{6} km^{2} (Holmes et al., 2012), more than 20% of continental Canada. It is the fourth-largest contributor of freshwater to the Arctic Ocean (330 km^{2}/yr) and by far the largest supplier of fluvial sediments (Fig. 1a), with about 128 Mt delivered to the delta annually (average 1974-1994; Carson et al., 1998). The Peel River contributes ca. 21 Mt/yr to this sediment load, and Arctic Red River ca. 7 Mt/yr. The Mackenzie River before the delta head receives most of its sediments from the Liard River that converges with the Mackenzie mainstem at Fort Simpson. The Liard River

supplies about 35-45 Mt/yr (Leitch et al., 2007) whereas the tributaries upstream of Fort Simpson contribute far less to the sediment load because Great Slave Lake acts as an efficient sediment trap (Carson et al., 1998). Nearly all sediment is delivered during May-October, with peak water discharge taking place in late May-early June when snow in the drainage basin melts. Later in the summer and autumn, several smaller peaks in discharge and sediment load occur during high rainfall events (Hill et al., 2001). About 13% and 29% of the watershed is underlain by continuous and discontinuous permafrost, respectively (Brown et al., 1998). The Mackenzie watershed has relatively low weathering rates and contains large amounts of sedimentary rocks (Dellinger et al., 2014). Three geological units occur in the Mackenzie River catchment (Millot et al., 2003): the North American Cordillera, the Interior Platform, and the Canadian Shield. The North American Cordillera (Proterozoic to Mesozoic age) is a tectonically active continental margin, located in the mountainous western part of the catchment (including headwaters of the Peel and Liard Rivers). The central Interior Platform (Cambrian to Cretaceous age) consists of sedimentary rocks at lower elevations (~500m). The old Precambrian Canadian Shield is drained by the far eastern part of the catchment, east of Lake Athabasca, Great Slave Lake and Great Bear Lake. Bedrock variability in the Mackenzie basin is said to be the major control for the geochemical and isotopic variability of fluvial sediments, rather than modern weathering processes (Dellinger et al., 2014).

The area of the Mackenzie River Delta is among northern deltas second only to the Lena River delta (Marsh et al., 1999). A vast number (>45,000; Emmerton et al., 2007) of small and shallow lakes occur in the delta, with sizes typically less than 10 ha in area and maximum depths of 4 m. It is estimated that these lakes hold ca. 47% of the spring flood water at peak discharge in late May/early June (Emmerton et al., 2007) and receive >60% of the annual sediment load during this short period (Carson et al., 1998). The gently rising topography from the Mackenzie River middle channel outwards to the east and west divides the delta lakes into no-closure, low-closure and high-closure lakes based on their flooding regime (Mackay, 1963; Lesack and Marsh, 2007). No-closure lakes (ca. 60% of total delta lake area) are permanently connected to a river channel. Low-closure lakes (ca. 25%) are only flooded during peak discharge in spring, become

disconnected later in summer and are isolated for the remainder of the year. High-closure lakes (ca. 15%) are only flooded in some years with exceptionally high water levels in spring. Sedimentation rates vary from ~1 to 10 mm/yr with generally increasing values from upper to lower delta and from high-closure lakes to no-closure lakes (Graf Pannatier, 1998; Marsh et al., 1999). The average lake sediment flux is between 1.2 and 5.3 kg/m^2/yr (Marsh et al., 1999), but as annual river-to-lake connection times have lengthened by >30 days over the last 30 years (Lesack and Marsh, 2007) this might slowly increase. Lake sediment deposition depends on the degree of closure (connectivity with main channel) and location relative to other lakes.

Sedimentation processes *within* the delta are not limited to delta lakes. Carson et al. (1999) provide a sediment balance diagram for the upper and outer delta. From the 128 Mt/yr arriving at the delta head (including the Peel River), they estimate that 85 Mt is transported offshore. Sediment redistribution in the delta gives rise to the net sedimentation of 43 Mt, as a result of ca. 102 Mt gross sedimentation combined with 59 Mt (bank) erosion within the delta. Consequently, the delta lakes most likely receive a mixed input from local sediment redistribution from other sedimentary settings (through e.g. erosion within the delta) and sediment sources further upstream (Mackenzie River downstream of Great Slave lake, Peel and Arctic Red Rivers).

Five major distributary channels discharge sediments from the Mackenzie Delta onto the Mackenzie shelf of the Canadian Beaufort Sea (Hill et al., 1991). The Mackenzie shelf is 100-150 km wide, has a fairly gentle relief and is ice-covered about six months per year. In contrast to the extensive Eurasian Arctic shelves, the Beaufort Sea continental shelf is relatively narrow bordering a relatively steep continental slope. The Mackenzie River is the major sediment source to the shelf, delivering about 90-95% of the sediments. Coastal erosion and rivers draining from Yukon Territory deliver the remainder of the sediment (Macdonald et al., 1998; Hill et al., 1991). Land-derived OC input accounts for >60% of the OC present in shelf sediments (Goñi et al., 2000; Yunker et al., 1995).

2.2 Sampling

198 Sediment cores (piston cores) were collected from lakes within the delta (Fig. 1c)
199 in late March/early April 2007 and late March 2009. Lakes were selected based
200 on satellite imagery, previous studies (Cordes and McLennan, 1984a,b; Marsh
201 and Hey, 1989; Graf Pannatier, 1998; Lesack et al., 1998; Marsh et al., 1999) and
202 ground penetrating radar surveys. Cores were collected from lakes that do not
203 freeze to the bottom (depth >3 m) to avoid sedimentary reworking by ice, and
204 coring sites were located distal from potential inflows or outflows. The cores
205 were shipped (unfrozen) to the Woods Hole Oceanographic Institution (WHOI;
206 US) and consequently split lengthwise in two using metal cutting shears,
207 wrapped and put into refrigerated storage. Sediment cores from four lakes in the
208 outer delta and two lakes in the lower delta were collected with a push corer
209 (Brown sampler) in March 1994 (Graf Pannatier, 1998). Core tops were sub-
210 sampled for analysis in February 2011.
211 Sediment samples from the Mackenzie shelf and Reindeer, East and Middle
212 channels (Fig. 1c and 1d) were collected as part of a large sampling program in
213 1987 in the Mackenzie River and Beaufort Sea using a Smith-McIntyre grab
214 sampler for the shelf samples and a Ponar grab sampler for the river samples. A
215 range of previous analyses on these samples has already been published (Yunker
216 et al. 1990, 1991, 1993; Goñi et al., 2000; 2005) but in this study we present only
217 new data.
218 Suspended particulate matter and bank sediments were collected during the
219 spring freshet in late May/early June 2011 (Fig. 1c). Surface water samples were
220 taken ca. 2.5 m from the shore or from mid-channel. Sediments at these channels
221 can exhibit rather large variability depending on water depth and width (e.g.,
222 Dellinger et al., 2014) such that the suspended samples collected here likely
223 represent the finest fraction. The samples were transported in coolers back to
224 the Aurora Research Station in Inuvik and filtered through 0.7 µm pre-
225 combusted GF/F filters (Whatman). The filtrates were subsampled for δ^2H and
226 $\delta^{18}O$ analyses, and stored cooled. The filters were stored and transported frozen
227 until further analyses. Bank sediments were manually collected at freshly
228 exposed banks (immediately after river levels lowered) with stainless steel
229 spoons. Cores of bank sediments in levees of lakes and channels in the lower
230 delta (levee in Fig. 1c) were collected in July 1993 (Graf Pannatier, 1998).

2.3 Sedimentological and mineralogical analyses

Organic matter was removed prior to particle-size and surface area analyses, by means of hydrogen peroxide and heating to 350°C (12 h), respectively (Keil et al., 1994; Keil et al., 1997). Particle-size analysis was performed on a Mastersizer 2000 (Malvern Instruments Ltd) laser-diffraction instrument (Geological Institute, ETH-Zürich) for particle size characterization from 0.02 to 2000 µm. The samples were dispersed in a 5 g/L Na-polyphosphate solution. Mineral surface area was determined on the whole samples (i.e. not size-fractionated) on a NOVA 4000e Surface Area Analyzer (Geological Institute, ETH-Zürich). Sample weight ranged from 1-5 g, based on known organic matter content, to secure sufficient surface area (>20 m^2) for a good measurement. After degassing at 420 °C for 12 hours, specific surface area was calculated through a 5-point BET measurement of relative pressure (P/P_0) based on adsorption.

For X-Ray Fluorescence (XRF) analyses, casting powders were prepared from a 1:5 mixture of lithium tetraborate (1.5 g) with dried and combusted (1050 °C, 1 h) sediment (7.5 g). The mixture was thoroughly ground with a mortar and pestle, and melted into pills with a Claisse M4 Fluxer. Analyses included 10 major and 21 minor/trace elements and were performed on a Panalytical Axios wavelength dispersive XRF spectrometer (WD-XRF) at the Institute of Geochemistry and Petrology (ETH-Zürich, Switzerland).

2.4 Isotope analyses

2.4.1 Stable carbon analysis

Dried sediment samples were analyzed for bulk OC content and stable carbon isotopic composition ($\delta^{13}C$) on a Carlo Erba/Fisons model 1108 Elemental Analyzer interfaced via a Conflo II to a Finnigan-MAT Delta^{Plus} isotope ratio mass spectrometry (IRMS; Marine Chemistry and Geochemistry Department, WHOI). Prior to analysis, samples were acid-treated to remove inorganic carbon according to the method described in Whiteside et al. (2011). Precision of analyses is about 0.11‰ (Table 1).

2.4.2 Radiocarbon analysis

Radiocarbon analysis was performed at the Laboratory of Ion Beam Physics, ETH-Zürich. Samples where acid-treated prior to analysis (Whiteside et al., 2011) and graphitized using an automated graphitization system (Wacker et al., 2010a). Samples were analyzed for ^{14}C using a MICADAS system (Wacker et al., 2010b) and calibrated again standard Oxalic Acid II (NIST SRM 4990C; precision of 3‰) and an in-house radiocarbon blank of anthracite coal. Precision of analyses is reported in Table 1.

2.4.3 Neodymium isotope analysis

A detrital inorganic fraction was isolated for geochemical characterization following sequential extraction procedures described in Bayon et al. (2002). Samples were spiked with ^{150}Nd and dissolved in a hydrofluoric/perchloric acid 4:1 mixture. Ion-exchange procedures with Ln-Spec resin were used, and isotope ratios were measured with a ThermoFinnigan NEPTUNE multi-collector inductively coupled plasma-mass spectrometer (MC-ICP-MS) at WHOI. The internal precision for Nd isotopic measurements is 15-25 ppm (two standard deviations). The external precision, after correction to values for LaJolla standards (0.511847), is approximately 15 ppm (two standard deviations). Sample heterogeneity also contributed to variability in the measurements, with an average ε–Nd difference of 0.68 units (n=5; standard deviation 0.35). For the samples in this study we will use an overall reproducibility of ±0.6 ε–Nd units.

2.4.4 Water isotope analysis

Water isotopes (δ^2H and $\delta^{18}O$) were analyzed using a Picarro L2120-i cavity-ringdown spectrometer (Geological Institute, ETH-Zürich) using VSMOW2, GISP and SLAP2 reference waters (International Atomic Energy Agency). Samples and reference waters were injected six times, while discarding the first two injections to eliminate instrumental memory effects.

3. RESULTS AND DISCUSSION

3.1 The Mackenzie delta as a sedimentary transition zone

3.1.1 Sorting and organic carbon loading

297 A river-to-shelf depositional sorting among sedimentary settings is clearly
298 visible as the sediment grain size generally decreases from the Mackenzie River
299 channels and banks to the Mackenzie delta lakes and the Mackenzie shelf (Fig. 2).
300 The Al/Si ratio (Fig. 3a) as a proxy for relative grain size (good correlation with
301 %clay; Fig. 3b) shows that bank and channel sediments are relatively quartz-rich
302 (lower Al/Si) and low in %OC, whereas lakes and shelf sediments are clay-rich
303 (higher Al/Si) and higher in %OC. The distinction based on Al/Si between bank
304 and channel sediments (Al/Si lower than ~0.23) versus lake and shelf sediments
305 (Al/Si >0.23) is very clear. Presumably this is a hydrodynamic sorting effect that
306 results in finer-grained sediments accumulating in lake and shelf deposits.
307 Hydrodynamic conditions also seem to affect the distribution of OC across the
308 delta. This relates to the differences in specific surface area between sediments
309 of different grain size, with fine sediments binding more OC than coarse
310 sediments (Fig. 3c and 3d). Suspended and bedload sediments of the Ganges-
311 Brahmaputra River and Amazon River, the largest rivers on Earth in terms of
312 sediment and water discharge, respectively, and far better characterized than
313 the Mackenzie River, show lower OC loadings compared to the Mackenzie (Fig.
314 4a) suggesting that the physical erosion characteristics in these rivers are
315 different than the Mackenzie. Grain size distribution is also clearly visible for
316 certain major elements such as K and Rb (Fig. 4b, d), elements that are abundant
317 in clay minerals, and also for Fe and Nd (not shown but data included in Table 3
318 and 4, respectively). Additionally, concentrations of Zr decrease with decreasing
319 grain size (higher Al/Si ratios; Fig. 4c; Table 4) except from a large variability in
320 bank sediments. Similar variability in Zr concentration was observed within the
321 coarse bed load of the Amazon and Ganges-Brahmaputra Rivers (Fig. 4c), likely
322 due to the relative enrichment of heavy minerals like zircon or rutile in the
323 coarse load (Bouchez et al., 2011).
324 The organic carbon to mineral surface area ratios (Fig. 3d) of Mackenzie
325 sediments fall within the range of 0.4-1.0 mg C/m^2, common for river-suspended
326 material and shelf sediments (Blair and Aller, 2012). This suggests that the
327 supply and decomposition of OC in the Mackenzie Delta is relatively balanced, in
328 contrast to systems with OC:SA ratios <0.4 mg C/m^2 (strong decomposition) or
329 >1.0 mg C/m^2 (strong supply or preservation/protection). Within the different

sample types, one can observe a general decrease of average organic carbon to mineral surface area (OC:SA) ratios with "depositional order": 1.1±0.4 mg C/m^2 for bank sediments (n=3), 0.95±0.3 for channel sediments (n=2), 0.84±0.2 for lake sediments (n=11), and 0.53±0.1 for shelf sediments (n=5) (Fig. 3d). The bank sediments we collected are located along the main stem, while channel and lake sediments are either farther downstream or farther in the channel diversion network, respectively. This could explain the decreasing OC:SA ratios through preferential deposition of the coarser fraction in the network, leading to a relatively higher surface area of sediments farther downstream. Suspended sediments collected during early and late freshet in 1987 near the delta front (Goñi et al., 2005) have an average OC:SA value of 0.78±0.06 mg C/m^2 (n=4; Fig. 3d). It is unlikely that the decrease in OC:SA is a dilution effect since biogenic debris contributions are small, as suggested by continuously high Al concentrations (Table 3) and minimal opal/carbonate material contributions on the shelf (<5 wt%, Goñi et al., 2000). The reduction in OC:SA values could be related to preferential transport of clay-sized particles with low OC contents (Fig. 3e and f) or mixing with OC-poor clays from the shelf. However, these data could also suggest a loss of mineral-bound terrestrial OC during transport through the delta and deposition on the shelf. Even within the subaqueous part of the delta, and the inner shelf, there is active OC loss as the stations closest to the river mouth show higher OC:SA values (0.59-0.61 mg C/m^2) than deeper stations further away from shore (0.43-0.54 mg C/m^2).

Parallel with a decrease in OC:SA ratios, we observe a gradual shift from terrestrial δ^{13}C-OC signatures towards more marine values on the shelf (Fig. 5a), along with decreasing C/N ratios (not shown) suggesting a simultaneous loss of riverine OC and replacement with marine OC throughout the delta (Keil et al., 1997; Yu et al., 2010). At the same time, there also appears to be a preferential loss of younger OC with decreasing OC:SA ratios (Fig. 5b). Given that there is a reasonable correlation between δ^{13}C and OC:SA (Fig. 5a) and Δ^{14}C and OC:SA (Fig. 5 b) the product of δ^{13}C and OC:SA against OC:SA (Fig. 5c) and likewise for Δ^{14}C (Fig. 5d) can be used to derive the net isotopic composition (δ^{13}C and Δ^{14}C) of OC lost from the sediments (Aller and Blair, 2006; Blair and Aller, 2012). This

suggests that the net value of terrestrial OC lost enroute is -28.5‰ for $\delta^{13}C$ and -417‰ for $\Delta^{14}C$ (Fig. 5c, d).

3.1.2 Burial efficiency

The decrease in organic carbon to mineral surface area ratios between river sediments and delta or shelf sediments (Fig. 3d) can be used to calculate the burial efficiency of organic matter. We here define the burial efficiency as the ratio of the amount of terrestrial OC that is buried on the shelf to what arrives at the delta head. Following the approach by Keil et al. (1997), burial efficiency of terrestrial OM on the Mackenzie shelf is determined by multiplying the fraction terrestrial OM (F-terr) with the fractional remaining surface loading (F-rsl) (Table 2). The F-terr is derived from stable carbon isotopic data:

$$\delta^{13}C_{shelf\ sediment} = \text{F-marine} \times \delta^{13}C_{marine} + \text{F-terr} \times \delta^{13}C_{river} \quad (1)$$

Here we use a $\delta^{13}C$ Mackenzie River value of -26.5 (river suspended sediments, n=4; Goñi et al., 2005) and a $\delta^{13}C$ marine value of -20.2‰ (Goñi et al., 2000). This gives an F-terr for shelf sediments of 67 to 98% (Table 2).

The F-rsl is derived from the decrease in mineral surface loading:

$$\text{F-rsl} = \text{OC:SA (shelf sample)} / \text{OC:SA (average bank samples)} \quad (2)$$

Here we use the average OC:SA of river suspended sediment samples (0.78 mg C/m^2; n=4; Goñi et al., 2005) that were collected in the East, Middle and Reindeer Channels. The F-rsl for nearshore shelf stations 5 and 13 is ~76%, giving a burial efficiency (i.e. F-rsl multiplied with F-terr) of ~71% (Table 2). Stations 9, SS2 and SS4, located farther away from the river mouth, have F-rsl values of 69%, 65% and 55%, respectively, and a burial efficiency around 45-51%. Overall, these estimates suggest that about 45% of the fluvial OM from Mackenzie River is lost during transport through the delta towards the shelf. The OC burial efficiency for the Mackenzie River (average±stdev 55±12%) appears to be higher than observed for tropical and temperate river systems (e.g. the Amazon, Fly and Columbia Rivers; Keil et al., 1997), which bury around 20-45% of their terrestrial

OM. This is probably due to a combination of cold temperatures and high accumulation rates in the Beaufort Sea along with the delivery of relatively pre-aged and pre-degraded OM. We should point out that our approach assumes that a reduction in OC:SA is related to a change in OC loading. If OC is not strongly related to grain size and is transported as discrete particles (macerals), our results would represent minimal estimates of burial efficiency.

3.2. Sediment provenance

3.2.1. Sediment OC age

Sediments in the Mackenzie Delta and adjacent Beaufort shelf are characterized by high contributions of both pre-aged biogenic OC and petrogenic OC. Bulk OC in bank sediments exhibited conventional ^{14}C ages between 6 and 13 ^{14}C-ky (for $\Delta^{14}C$ values see Table 1). Corresponding values for channel sediments were 6 to 8.5 ^{14}C-ky, and 1.9 to 12 ^{14}C-ky for lake sediments. Shelf sediments were between 5.1 and 12 ^{14}C-ky (stations 13, 23, 29), which is in the same range as the ^{14}C ages of the other stations published previously (Table 1, Goñi et al., 2005; Drenzek et al., 2007). Organic carbon in suspended river sediments was also old, with values of 6.6 ^{14}C-ky (Tsiigehtchic; Table 1), and 7.2 to 10 ^{14}C-ky (East, Middle and Reindeer channels outer delta; Goñi et al., 2005). Prior to ice break-up, suspended matter collected under-ice is younger (2.9 ^{14}C-ky; East Channel near Inuvik, May 27, 2011) yet still showing signs of relict OC contributions. Old sedimentary OC ages most likely point at a significant contribution of relict, petrogenic source rock material (possibly from the Devonian Canol formation that outcrops in the lower Mackenzie River valley; Yunker et al., 1993; 2002), along with pre-aged terrestrial OC from either recalcitrant soil OM, paleosols, or thawing permafrost soils (Drenzek et al., 2007).

3.2.2. Inputs of biogenic versus petrogenic OC

Stable carbon isotope values (Fig. 6a) suggest a dominant terrestrial source in the subaerial delta and a gradual dilution with marine OM on the nearshore Mackenzie shelf. Lake sediments with %OC contents above ~2%, appear to receive some of their OC from younger sources (Fig. 6a) and show a high variability in $\delta^{13}C$ signatures (-23.5 to -30.7‰). Most likely these lakes receive a

higher than average input from fresh allochthonous material (e.g. peat -26‰; Goñi et al., 2000) or autochthonous material (ranging between -19 to -34‰, depending on timing of bloom; Tank et al., 2011). Note that all high-closure lakes fall within this "cluster" of young, high OC% sediments (see section 3.3). High-closure lakes only receive sediments on an occasional basis, are clearer and most likely have a higher algal and macrophyte productivity, suggesting that these lakes have a higher autochthonous input to their sediment.

Based on a simple two end-member mixing model ($\Delta^{14}C$ modern OC 0‰, $\Delta^{14}C$ ancient OC -1000‰) Goñi et al. (2005) estimated the ancient OC contribution to be 59-88% for shelf sediments and 59-71% for outer delta suspended matter sediments. A similar approach for our sampling stations gives an ancient OC contribution of 61±13% and 63±4% for bank and channel sediments, respectively, 67±4% for low-OC lakes (53±21% for all lakes) and 67±9% for shelf sediments. Suspended particulate matter has a lower but still considerable contribution of ancient OM of 57%. However, defining modern or biospheric OM with a $\Delta^{14}C$ of 0‰ is not entirely valid, as biospheric OM consists of a large mixture of sources (some of it pre-aged; Kuhry and Vitt, 1996). Also, the definition of "ancient OM" is likely too simplistic; differentiating between a petrogenic source ($\Delta^{14}C$ -1000‰) and a pre-aged terrestrial source (anything between $\Delta^{14}C$ modern and -1000‰) would be preferred, but not possible based on only bulk measurements. Drenzek et al. (2007) used both bulk and molecular ^{14}C and ^{13}C analyses to circumvent this issue. They estimated the average total terrestrial contribution on the Mackenzie shelf (station 5 and 9; Fig. 1b) to be roughly equally split between pre-aged terrestrial OC and petrogenic OC (~44% for each) with the remainder (~13%) being marine.

An alternative approach uses Al/OC_{total} ratios in combination with Fm values (Fig. 6b; Bouchez et al., 2014; Dellinger et al., 2014) to derive the age of biogenic OC in Mackenzie River sediments along with the fraction petrogenic (F-petrogenic) and fraction biogenic (F-biogenic) OC. By using the intercept at Fm = 0 to calculate the Al/OC ratio of petrogenic bedrock (Fig. 6b) this gives a $Al/OC_{petrogenic}$ ratio of around 120000. We then used the Al content (ppm) of Mackenzie bedload samples (average 31700 ppm, n=4; Dellinger et al., 2014) to calculate an $\%OC_{petrogenic}$ of 0.26%. We assume that $\%OC_{petrogenic}$ is relatively

461 constant in the delta (Galy et al., 2007; Galy et al., 2011), at least compared with
462 biogenic OC, and then use the %OC of the sample and $\%OC_{petrogenic}$ to calculate F-
463 petrogenic. Using equation (3) one can then derive the $Fm_{biogenic}$.
464 $F\text{-biogenic} \times Fm_{biogenic} + F\text{-petrogenic} \times Fm_{petrogenic} = Fm_{sample}$ (3)
465
466 Where F-biogenic = (1-F-petrogenic), since F-petrogenic is known, and
467 $Fm_{petrogenic} = 0$. This gives F-petrogenic values of 19±9% and an average $\Delta^{14}C$ of
468 biogenic OC (Fig. 6c; Bouchez et al., 2014) for shelf, lake, bank, channel and
469 suspended sediments of -501‰ (standard deviation 186‰; n=35)
470 corresponding to an average age of about 6100 ^{14}C-yrs. The fraction petrogenic
471 is now obviously lower than calculated above (57-67%) as the biogenic
472 component is much older than we assumed previously (0‰). The calculated
473 biogenic OC ^{14}C-signal is somewhat older than the terrestrial $\Delta^{14}C$ signal of -
474 417‰ that is calculated to be lost during transport through the delta (Fig. 5d).
475 Several previous studies using biomarkers and bulk organic properties (e.g.,
476 Yunker et al., 1993; 2002; Goñi et al., 2005) have shown that fossil petrogenic OC
477 contributes to Mackenzie sediments, but the presence of a substantial, pre-aged
478 biogenic OC component has not been shown before. Our results suggest that
479 terrestrial OC resides for millennia in soils before being released to the river.
480
481 **3.3 Sediment and source rock patterns within the delta**
482 *3.3.1. Neodymium isotopes as tracers of source rocks*
483 A wide range of studies have used Nd isotopes to trace or fingerprint ocean
484 circulation patterns and river input (Porcelli et al., 2009; Andersson et al., 1992;
485 Öhlander et al., 2000), weathering processes (Andersson et al., 2001), and dust
486 and sediment provenance (Grousset and Biscaye, 2005; Meyer et al., 2011). In
487 the Arctic, Nd isotopic signatures of river water (dissolved load) range between -
488 5 and -41 (Table 5 and references therein), reflecting major difference in
489 bedrock age and composition of river catchments.
490 The Nd isotopic compositions of the siliciclastic fraction of surface suspended
491 sediments from different rivers/tributaries delivered to the Mackenzie delta
492 (June 2011) range between -11.6 and -13.9 (ε units) whereas bank, lake and
493 shelf sediments range between -12.4 and -14.5 (Table 3, Fig. 7 and 8a). These

494 ranges are distinctly larger than the analytical uncertainty (0.49 ε units) or
495 sample reproducibility (0.68 ε units). Lake surface sediments also show a fairly
496 large variability (-11.2 to -14.5) in ε□□□but, in contrast with the other sample
497 types, exhibit a gradual but distinct spatial transition from the western to the
498 eastern delta (Fig. 7a). In the west the younger, more radiogenic signals point
499 towards input from the younger Peel River catchment draining the tectonically
500 active North American Cordillera. In the east, Nd signals in lake surface
501 sediments are less radiogenic suggesting a higher input of older geological
502 source regions such as the Interior Platform, the Devonian Canol formation as
503 mentioned previously (Yunker et al., 1993; 2002) or even the Precambrian
504 Canadian Shield. We reason that the lack of spatial patterns in suspended, bank
505 and channel sediments can be attributed to different factors associated with, for
506 example, grain size, timing of sampling and/or timing of deposition, and annual
507 variability. The gradual but significant transition towards a younger Peel-like
508 source observed in lakes from east to west suggests that lake sediments are
509 homogenized and represent a long-term integrated signal.
510 A primary factor likely affecting the large variability in Nd isotopic signatures is
511 grain size. This is a key sediment property that is indicative for the
512 hydrodynamic regime; fine sediments remain in the suspended load and can
513 travel faster/farther, while coarse sediments will mostly travel slower as bed
514 load for shorter distances. Bed load is also more likely to be influenced by
515 sources closer to the delta due to the time lag introduced by bed load transport.
516 Depending on flow regime, sediments from the same source region but with
517 different grain sizes can therefore be deposited at different locations along the
518 land-to-ocean pathway. We see here that coarser sediments (bank sediments)
519 have lower εNd values, i.e. are less radiogenic (Fig. 7b, 8c) compared with finer
520 SPM and lake sediments from the same region. Possibly, the Liard River
521 catchment, located more than 1000 km upstream from the delta head and
522 consisting of relatively young source rocks, contributes more to the fine load
523 (SPM and lake sediments), explaining its relatively young εNd signal. The grain-
524 size dependency of εNd that we observe is in contrast with some previous
525 studies (e.g. Garçon et al., 2013).

Also, the timing of sampling in an Arctic river with an extremely seasonal discharge, such as the Mackenzie can strongly influence the sample properties. We collected SPM samples during a two-week period in May-June 2011 when the bulk of the annual sediment load was delivered. Each sampled tributary however is at a different stage of the annual hydrological profile, due to differences in relief, elevation and latitude, as can be illustrated by the rather large range in river water hydrogen isotopic signatures (Fig. 9) and their variability during the sampling period. These shifts in water isotopes represent the shift in water flow paths from surface to subsurface flow in spring as the water source transitions from snow to groundwater (e.g. Voss et al., 2014). Likewise, water flow path shifts are indicators of differences in erosion-derived sediment sources with different εNd signatures.

Thirdly, annual variability in the level and "slope" of the spring flood peak affects the (timing of) sediment deposition, particularly in delta lakes. For example, a year with a very early and abrupt river level rise might cause significant overbank flooding and/or sediment delivery upon ice-covered lakes, whereas a more gradual rise of the spring peak will push more (and different) sediments through delta channels. Overbank flooding and channel diversions likely also depend on ice jamming. In lake LD-1, the 1994 and 2007 core tops show comparable values for $\delta^{13}C$, $\Delta^{14}C$, %clay, and mineral surface area (Table 1), while their Nd values are distinctly different (1994: -13.9, 2007: -11.2; Table 3; Figure 8d). Lakes were sampled in March so the sediment originated in the previous summer. The strong difference in peak flood levels in the years prior to sampling (1993: 12.5 m, 2006: 19.5 m; hydrometric station at Arctic Red River/Mackenzie, Goulding et al., 2009) could potentially explain part of this contrast, together with the timing and intensity of rising water levels (1993: water level May 23 7.5m - May 31 10.5 m; 2006: May 13 7.8 m – May 22 19.4 m; www.ec.gc.ca, station 10LC014).

Carson et al. (1999) estimate that bank erosion in the delta redistributes about 59 Mt of sediment annually. We observe (Fig. 8b and 8c) that fine sediments have higher concentrations of Nd and more radiogenic ε_{Nd} signals, while coarse sediments contain less Nd and are less radiogenic (i.e. older in Nd terms). This could partly be a dilution effect through higher amounts of, for example, quartz

559 in the coarse sediments. However, this can also be explained by the delivery of a
560 local sediment source, from, for example, bank erosion, as Carson et al. (1999)
561 suggested. The sediment Nd patterns (fine and young vs. coarse and old)
562 contrast with what we would have expected based on the vicinity of source areas
563 versus sediment delivery: Peel and Arctic Red rivers are nearby and are
564 therefore expected to deliver more of the coarse load, from watersheds that
565 drain relatively young source rocks. Much of the material from the Mackenzie
566 mainstem, on the other hand, originates from farther South and is therefore
567 expected to favor finer sediments from relatively old source rocks. We
568 hypothesize that this grain size-age contrast can be explained by sediment
569 erosion *within* the delta. That is, erosion of fine sediments with younger, more
570 radiogenic Nd from levees and/or erosion of coarser sediments with older, less
571 radiogenic Nd from bank sediments could account for this discrepancy.
572
573 *3.3.2 Patterns with degree of lake closure*
574 The Mackenzie Delta is a fascinating environment with a whole array of complex
575 channel-lake connections. Every single lake of the >45,000 lakes (Emmerton et
576 al., 2007) is unique. Interpreting sediment deposition patterns based solely on
577 the commonly used classification system of no-closure, low-closure and high-
578 closure lakes is not adequate as, for example, interannual variability and a strong
579 heterogeneity in lake-channel connectivity (illustrated in Fig. 10) are important
580 complicating factors. Explaining patterns in sedimentary characteristics between
581 delta lakes is therefore challenging. For example, the *degree* of river-lake
582 connection differs from year-to-year for high-closure lakes, whereas the *length* of
583 this river-lake connection differs from year-to-year for low-closure lakes. The
584 relative distance to the major sediment source also varies, along with the
585 number of intermediate settling basins. Lake MD-9, for example, is connected via
586 two channels and another lake to the Mackenzie main branch, whereas UD-1 is
587 directly connected with a channel to a major Mackenzie side branch. Also, the
588 means of sediment delivery (e.g., overbank flooding versus channel inflow) is
589 important, and the relative input of bank or levee erosion versus river sediment
590 delivery. Nevertheless, one can see that high-closure lakes hold relatively high
591 OC contents and young biogenic OC (Fig. 11a and 11b), originating either from

592 terrestrial ($\delta^{13}C$ around -27‰) or autochthonous ($\delta^{13}C$ around -23.5‰)
593 sources. Low-closure lakes also seem to receive a range of OC sources ($\delta^{13}C$
594 between -24.5‰ and -28.5‰) whereas no-closure lakes, presumably with
595 higher turbidities as they are continuously connected to the river, are dominated
596 by terrestrial inputs ($\delta^{13}C$ around -27.5‰). Grain size (not shown) does not
597 seem to show any clear differences among lake types.
598
599 **3. CONCLUSIONS**
600 The Mackenzie delta is one of the largest deltas in the Arctic, receiving about 128
601 Mt of fluvial sediments every year. Sediment grain size and OC to mineral surface
602 area ratios generally decrease from channel and bank sediments to lake and
603 shelf sediments, suggesting depositional sorting patterns. We calculated that
604 only about 55% of the incoming sedimentary OC is buried on the coastal shelf,
605 suggesting a loss of 45% in the delta. The sedimentary OC consists of a
606 petrogenic source contribution of 19±9% when using a derived ^{14}C-signature of
607 pre-aged biogenic OC of -501‰). Grain size, interannual variability and timing of
608 sampling hinder the detection of spatial (delta-wide) trends when using εNd
609 signatures in suspended, bank and channel sediments. Lake surface sediment
610 εNd results, however, show a gradual transition from west (younger source
611 rocks) to east (older source rocks) in the delta suggesting that Mackenzie delta
612 lakes represent a homogenized temporally-integrated signal.
613
614 *Acknowledgements* – We would like to acknowledge financial support from the
615 WHOI Arctic Research Initiative, the US NSF Arctic Natural Sciences (ARC
616 #0909377), the US NSF Arctic GRO (#0732522 and #1107774), NWO Rubicon
617 (#825.10.022) and NWO Veni (#863.12.004), and ETH Zürich. Furthermore, we
618 would like to thank Maria-Louisa Tavagna, Tessa van der Voort, Negar
619 Haghipour, Lydia Zehnder, Stefanie Wirth, Britta Voss, Carl Johnson, Irka Hajdas
620 and Claire Griffin for their help with analyses, discussion and fieldwork.
621 Furthermore, we thank people that helped with Mackenzie winter sampling
622 (Angela Dickens, David Griffith, Camilo Ponton, Valier Galy, and Rebecca Sorell)
623 and core analysis (Samuel Zipper). We also thank the Institute F.-A. Forel
624 (Geneva, Switzerland) for archiving samples, and the Aurora Research Institute

(Inuvik, Canada) and helicopter companies Canadian Helicopter and Highland North Helicopter for logistical support.

REFERENCES

Aller R. C. and Blair N. E. (2006) Carbon remineralization in the Amazon-Guianas tropical mobile mudbelt: a sedimentary incinerator. *Cont. Shelf. Res.* **26**, 2241-2259.

Andersson P. S., Wasserburg G. J., and Ingri J. (1992) The sources and transport of Sr and Nd isotopes in the Baltic Sea. *Earth Planet. Sci. Lett*. **113**, 459-472.

Andersson P. S., Dahlqvist R., Ingri J., and Gustafsson Ö. (2001) The isotopic composition of Nd in a boreal river: A reflection of selective weathering and colloidal transport. *Geochim. Cosmochim. Acta* **65**, 521-527.

Andersson P., Guo L., Semiletov I., Gustafsson Ö., Ingri J., Dudarev O., and White D. (2003) Nd- and Sr isotopes in Siberian Arctic estuarine sediments: implications for sediment provenance. EGS-AGU-EGU Joint Assembly, abstract #5475.

Asahara Y., Takeuchi F., Nagashima K., Harada N., Yamamoto K., Oguri K., and Tadai O. (2012) Provenance of terrigenous detritus of the surface sediments in the Bering and Chukchi Seas as derived from Sr and Nd isotopes: Implications for recent climate change in the Arctic regions. *Deep-Sea Res. Pt II* **61-64**, 155-171.

Bayon G., German C.R., Boella R.M., Milton J.A., Taylor R.N., Nesbitt R. W. (2002) An improved method for extracting marine sediment fractions and its application to Sr and Nd isotopic analysis. *Chem. Geol.* **187**, 179 - 199.

Bianchi T. S., and Allison M. A. (2009) Large-river delta-front estuaries as natural "recorders" of global environmental change. *P. Natl. Acad. Sci. USA* **106**, 8085-8092.

Blair N.E., and Aller R.C. (2012) The fate of terrestrial organic carbon in the marine environment. *Annu. Rev. Mar. Sci.* **4**, 401-423.

Bouchez J., Gaillardet J., France-Lanord C., Maurice L., and Dutra-Maia P. (2011) Grain size control of river suspended sediment geochemistry: Clues from Amazon River depth profiles. *Geochem. Geophys. Geosyst*. **12**, Q03008, doi:10.1029/2010GC003380.

Bouchez J., Galy V., Hilton R. G., Gaillardet J., Moreira-Turcq P., Andrea Perez A., France-Lanord C., and Maurice L. (2014) Source, transport and fluxes of Amazon River particulate organic carbon: Insights from river sediment depth-profiles. *Geochim. Cosmochim. Acta* **133**, 280-298.

Brown J., Ferrians O. J. Jr., Heginbottom J. A., and Melnikov E. S. (1998) Circum-arctic Map of Permafrost and ground ice conditions. National Snow and Ice Data Center. Boulder (CO), US.

Burdige D. J. (2005) Burial of terrestrial organic matter in marine sediments: A re-assessment. *Global Biogeochem. Cycles* **19**, GB4011, doi:10.1029/2004GB002368.

Carson M. A., Malcolm Conly F., and Jasper J. N. (1999) Riverine sediment balance of the Mackenzie Delta, Northwest Territories, Canada. *Hydrol. Process.* **13**, 2499-2518.

671 Carson M. A., Jasper J. N., and Conly F. M. (1998) Magnitude and sources of
672 sediment input to the Mackenzie Delta, Northwest Territories, 1974-94. *Arctic*
673 **51**, 116-124.
674 Cohen S. J. (1997) What if and so what in Northwest Canada: Could climate
675 change make a difference to the future of the Mackenzie Basin? *Arctic* **50**, 293-
676 307.
677 Cordes L.D., and McLennan D.S. (1984a) Bathymetry and morphometry of 32
678 Mackenzie Delta Lakes. British Columbia Power and Hydro Authority Report,
679 1-35.
680 Cordes L.D., and McLennan D.S. (1984b) The estimation of sedimentation rates
681 using ^{137}Cs in lakes of the Mackenzie Delta. British Columbia Power and Hydro
682 Authority Report, 1-55.
683 Dellinger M., Gaillardet J., Bouchez J., Calmels D., Galy V., Hilton R.G., Louvat P.,
684 and France-Lanord C. (2014) Lithium isotopes in large rivers reveal the
685 cannibalistic nature of modern continental weathering and erosion. *Earth*
686 *Planet. Sci. Lett*. **401**, 359-372.
687 Déry, S. J., Hernández-Henriquez, M. A., Burford, J. E., and Wood, E. F. (2009)
688 Observational evidence of an intensifying hydrological cycle. *Geophys. Res.*
689 *Lett*. **36**, L13402, doi:10.1029/2009GL038852.
690 Drenzek N. J., Montlucon D. B., Yunker M. B., Macdonald R. W., and Eglinton T. I.
691 (2007) Constraints on the origin of sedimentary organic carbon in the
692 Beaufort Sea from coupled molecular 13C and 14C measurements. *Mar. Chem.*
693 **103**, 146-162.
694 Emmerton C. A., Lesack L. F. W., and Marsh P. (2007) Lake abundance, potential
695 water storage, and habitat distribution in the Mackenzie River Delta, western
696 Canadian Arctic. *Water Resour. Res.* **43**, W05419.
697 Galy V., France-Lanord C., Beyssac O., Faure P., Kudrass H., and Palhol F. (2007)
698 Efficient organic carbon burial in the Bengal fan sustained by the Himalayan
699 erosional system. *Nature* **450**, 407-417.
700 Galy V., France-Lanord C., and Lartiges B. (2008) Loading and fate of particulate
701 organic carbon from the Himalaya to the Ganga-Brahmaputra delta. *Geochim.*
702 *Cosmochim. Acta* **72**, 1767-1787.
703 Galy V., and Eglinton T. (2011) Protracted storage of biospheric carbon in the
704 Ganges-Brahmaputra basin. *Nat. Geosci*. **4**, 843-847.
705 Garçon M., Chauvel C., France-Lanord C., Huyghe P., and Lavé J. (2013)
706 Continental sedimentary processed decouple Nd and Hf isotopes. *Geochim.*
707 *Cosmochim. Acta* **121**, 177-195.
708 Goldstein S.L., O'Nions R.K., and Hamilton P.J. (1984) A Sm-Nd isotopic study of
709 atmospheric dusts and particulates from major river systems. *Earth Planet.*
710 *Sci. Lett*. **70**, 221-236.
711 Goldstein S.J., and Jacobsen S.B. (1988) Nd and Sr isotopic systematics of river
712 water suspended material: implications for crustal evolution. *Earth Planet. Sci.*
713 *Lett*. **87**, 249-265.
714 Goñi M. A., Yunker M. B., Macdonald R. W., and Eglinton T. I. (2000) Distribution
715 and sources of organic biomarkers in arctic sediments from the Mackenzie
716 River and Beaufort Shelf. *Mar. Chem.* **71**, 23-51.
717 Goñi M. A., Yunker M. B., Macdonald R. W., and Eglinton T. I. (2005) The supply
718 and preservation of ancient and modern components of organic carbon in the
719 Canadian Beaufort Shelf of the Arctic Ocean. *Mar*. *Chem*. **93**, 53-73.

720 Gordeev V. V. (2006) Fluvial sediment flux to the Arctic Ocean. *Geomorphology*
721 **80**, 94-104.
722 Goulding H. L., Prowse T. D., and Bonsal, B. (2009) Hydroclimatic controls on the
723 occurrence of break-up and ice-jam flooding in the Mackenzie Delta, NWT,
724 Canada. *J. Hydrol.* **379**, 251-267.
725 Graf Pannatier E. (1998) Sediment accumulation and historical deposition of
726 trace metals and trace organic compounds in the Mackenzie Delta (Northwest
727 Territories, Canada). Thesis, University of Geneva, Switzerland.
728 Griffith D. R., McNichol A. P., Xu L., McLaughlin F. A., Macdonald R. W., Brown K.
729 A., and Eglinton T. I. (2012) Carbon dynamics in the western Arctic Ocean:
730 insights from full-depth carbon isotope profiles of DIC, DOC, and POC.
731 *Biogeosciences* **9**, 1217-1224.
732 Grousset F. E., and Biscaye P. E. (2005) Tracing dust sources and transport
733 patterns using Sr, Nd and Pb isotopes. *Chem. Geol.* **222**, 149-167.
734 Guo L., Semiletov I., Gustafsson Ö., Ingri J., Andersson P., Dudarev O., and White D.
735 (2004) Characterization of Siberian Arctic coastal sediments: Implications for
736 terrestrial organic carbon export. *Global Biogeochem. Cycles* **18**, GB1036,
737 doi:10.1029/2003GB002087.
738 Guo L., Ping C.-L., and Macdonald R. W. (2007) Mobilization pathways of organic
739 carbon from permafrost to arctic rivers in a changing climate. *Geophys. Res.*
740 *Lett.* **34**, L13603, doi:10.1029/2007GL030689.
741 Hill P. R., Blasco S. M., Harper J. R., and Fissel D. B. (1991) Sedimentation on the
742 Canadian Beaufort Shelf. *Cont. Shelf. Res.* **11**, 821-842.
743 Hill P. R., Lewis C. P., Desmarais S., Kauppaymuthoo V., and Rais H. (2001) The
744 Mackenzie Delta: sedimentary processes and facies of high-latitude, fine-
745 grained delta. *Sedimentology* **48**, 1047-1078.
746 Holmes R. M., McClelland J. W., Peterson B. J., Shiklomanov I. A., Shiklomanov A. I.,
747 Zhulidov A. V., Gordeev V. V., and Bobrovitskaya N. N. (2002) A circumpolar
748 perspective on fluvial sediment flux to the Arctic Ocean. *Global Biogeochem.*
749 *Cycles* **16**, 1098, doi:10.1029/2001GB001849.
750 Holmes R. M., McClelland J. W., Peterson B. P., Tank S. E., Bulygina E., Eglinton T.
751 I., Gordeev V. V., Gurtovaya T. Y., Raymond P. A., Repeta D. J., Staples R., Striegl
752 R. G., Zhulidov A. V., and Zimov S. A. (2012) Seasonal and annual fluxes of
753 nutrients and organic matter to the Arctic Ocean and surrounding seas,
754 *Estuar. Coasts* **35**, 369-382.
755 Jenner, K. A., and Hill, P. R. (1991) Sediment transport at the Mackenzie Delta-
756 Beaufort Sea interface. In Mackenzie Delta: Environmental Interactions and
757 Implications of Development, Marsh P., Ommanney C. S. L. (eds), National
758 Hydrology Research Institute, Environment Canada: Saskatoon,
759 Saskatchewan.
760 Keil, R. G., Mayer, L. M., Quay, P. D., Richey, J. E., and Hedges, J. I. (1997) Loss of
761 organic matter from riverine particles in deltas. *Geochim. Cosmochim. Acta* **61**,
762 1507-1511.
763 Keil, R. G., Tsamakis, E. C., Fuh, C. B., Giddings, J. C., and Hedges, J. I. (1994)
764 Mineralogical and textural controls on the organic composition of coastal
765 marine sediments: Hydrodynamic separation using SPLITT-fractionation
766 *Geochim. Cosmochim. Acta* **58,** 879-893.
767 Kuhry, P., and Vitt, D. H. (1996) Fossil carbon/nitrogen ratios as a measure of
768 peat decomposition. *Ecology* **77**, 271-275.

769 Leitch, D. R., Carrie, J., Lean, D., Macdonald, R. W., Stern, G. A., and Wang, F. (2007)
770 The delivery of mercury to the Beaufort Sea of the Arctic Ocean by the
771 Mackenzie River. *Sci. Total Environ.* **373**, 178-195.
772 Lesack, L. F. W, and Marsh, P. (2007) Lengthening plus shortening of river-to-
773 lake connection times in the Mackenzie River Delta respectively via two global
774 change mechanisms along the arctic coast. *Geophys. Res. Lett.* **34**, L23404.
775 Lesack, L.F.W., Marsh, P., Hecky, R.E. (1998) Spatial and temporal dynamics of
776 major solute chemistry among Mackenzie Delta lakes. Limnol. Oceanogr. 43,
777 1530-1543.
778 Lesack, L. F. W., Marsh, P., Hicks, F. E., and Forbes, D. L. (2014) Local spring
779 warming drives earlier river-ice breakup in a large Arctic delta. *Geophys. Res.*
780 *Lett.* **41**, 1560-1566.
781 Macdonald, R. W., Solomon, S. M., Cranston, R. E., Welch, H. E., Yunker, M. B., and
782 Gobeil, C. (1998) A sediment and organic carbon budget for the Canadian
783 Beaufort Shelf. *Mar. Geol.* **144**, 255-273.
784 Macdonald, R. W., Iseki, K., O'Brien, M. C., McLaughlin, F. A., McCullough, S.,
785 Macdonald, D. M., Carmack, E. C., Yunker, M., Buckingham, S., and Miskulin, G.
786 (1998) NOGAP B.6; Volume 5: Chemical data collected in the Beaufort Sea and
787 Mackenzie River delta March-July 1987. Canadian Data Report of
788 Hydrography and Ocean Sciences No. 60. 56 pp.
789 Mackay, J. R. (1963) The Mackenzie Delta area, NWT. Geographical Branch
790 Memoir No. 8: Ottawa, Canada.
791 Marsh, P. and Hey M. (1989) The flooding hydrology of Mackenzie Delta Lakes
792 near Inuvik, N.W.T. Canada. Arctic 42, 41-49.
793 Marsh, P., Lesack, L. F. W., and Roberts, A. (1999) Lake sedimentation in the
794 Mackenzie Delta, NWT. *Hydrol. Process.* **13**, 2519-2536.
795 Meyer, I., Davies, G. R., and Stuut, J.-B. W. (2011) Grain size control on Sr-Nd
796 isotope provenance studies and impact on paleoclimate reconstructions: And
797 example from deep-sea sediments offshore NW Africa. *Geochem. Geophys.*
798 *Geosyst*. 12, Q03005, doi:10.1029/2010GC003355
799 Millot, R., Gaillardet, J., Dupré, B., and Allègre, C. J. (2003) Northern latitude
800 chemical weathering rates: Clues from the Mackenzie River Basin, Canada.
801 *Geochim. Cosmochim. Acta* **67**, 1305-1329.
802 Oelke, C., Zhang, T., and Serreze, M.C. (2004) Modeling evidence for recent
803 warming of the Arctic soil thermal regime. *Geophys. Res. Lett.* **31**, L07208,
804 doi:10.1029/2003GL019300.
805 Öhlander, B., Ingri, J., Land, M., Schöber, H. (2000) Change of Sm-Nd isotope
806 composition during weathering of till. *Geochim. Cosmochim. Acta* **64**, 813-820.
807 Overeem, I., and Syvitski, J. P. M. (2010) Shifting discharge peaks in Arctic rivers,
808 1977-2007. *Geogr. Ann* **92** A, 285-296.
809 Peterson, B. J., Holmes, R. M., McClelland, J. W., Vorosmarty, C. J., Lammers, R. B.,
810 Shiklomanov, A. I., Shiklomanov, I. A., Rahmstorf, S. (2002) Increasing river
811 discharge to the Arctic Ocean. *Science* **298**, 2171-2173.
812 Porcelli, D., Andersson, P. S., Baskaran, M., Frank, M., Björk, G., and Semiletov, I.
813 (2009) The distribution of neodymium isotopes in Arctic Ocean basins.
814 *Geochim. Cosmochim. Acta* **73**, 2645-2659.
815 Schreiner, K. M., Bianchi, T. S., Eglinton, T. I., Allison, M. A., and Hanna, A. J. M.
816 (2013) Sources of terrigenous inputs to surface sediments of the Colville River
817 Delta and Simpson's Lagoon, Beaufort Sea, Alaska. *J. Geophys. Res.-Biogeo.* **118**,

808-824.
Smith, S. L., Burgess, M. M., Riseborough, D., and Nixon, F. M. (2005) Recent trends from Canadian permafrost thermal monitoring network sites. *Permafrost and Periglac. Process.* **16**, 19-30.
Tank, S. E., Lesack, L. F. W., Gareis, J. A. L., Osburn, C. L., and Hesslein, R. H. (2011) Multiple tracers demonstrate distinct sources of dissolved organic matter to lakes of the Mackenzie Delta, western Canadian Arctic. *Limnol. Oceanogr.* **56(4)**, 1297-1309.
VanLaningham, S., Pisias, N. G., Duncan, R. A., and Clift, P. D. (2009) Glacial-interglacial sediment transport to the Meiji Drift, northwest Pacific Ocean: Evidence for timing of Beringian outwashing. *Earth Planet Sc. Lett.* **277**, 64-72.
Voss, B. M., Peucker-Ehrenbrink, B., Eglinton, T. I., Fiske, G., Wang, Z. A., Hoering, K. A., Montlucon, D. B., LeCroy, C., Pal, S., Marsh, S., Gillies, S. L., Janmaat, A., Bennett, M., Downey, B., Fanslau, J., Fraser, H., Macklam-Harron, G., Martinec, M., and Wiebe, B. (2014) Tracing river chemistry in space and time: Dissolved inorganic constituents of the Fraser River, Canada. *Geochim. Cosmochim. Acta* **124**, 283-308.
Wacker, L., Nemec, M., and Bouquin, J. (2010a) A revolutionary graphitisation system: Fully automated, compact and simple. *Nucl. Instrum. Meth B* **268**, 931-934.
Wacker, L., Bonani, G., Friedrich, M., Hajdas, I., Kromer, B., Nemec, M., Ruff, M., Suter, M., Synal, H.-A., and Vockenhuber, C. (2010b) MICADAS: Routine and High-precision radiocarbon dating. *Radiocarbon* **52**, 252-262.
Whiteside, J. H., Olsen, P. E., Eglinton, T. I., Cornet, B., McDonald, N. G., and Huber, P. (2011) Pangean great lake paleoecology on the cusp of the end-Triassic extinction. *Palaeogeogr. Palaeoclimat. Palaeoecol.* **301**, 1-17.
Yu, F., Zong, Y., Lloyd, J. M., Huang, G., Leng, M. J., Kendrick, C., Lamb, A. L., and Yim, W. W.-S. (2010) Bulk organic d13C and C/N as indicators for sediment sources in the Pearl River delta and estuary, southern China. *Estuar. Coast. Shelf. Sci.* **87**, 618-630.
Yunker, M.B., et al. (1990), NOGAP B.6; Volume 7: Hydrocarbon determinations; Mackenzie River and Beaufort Sea shoreline peat samples, Canadian Data Report of Hydrography and Ocean Sciences 60, 1-81.
Yunker, M.B., et al. (1991), Geochemistry and fluxes of hydrocarbons to the Beaufort Sea shelf: A multivariate comparison of fluvial inputs and shoreline erosion of peat using principal components analysis, *Geochim. Cosmochim. Ac.* 55, 255-273.
Yunker, M. B., Macdonald, R. W., Cretney, W. J., Fowler, B. R., and McLaughlin, F. A. (1993) Alkane, terpene and polycyclic aromatic hydrocarbon geochemistry of the Mackenzie River and Mackenzie shelf: Riverine contributions to Beaufort Sea coastal sediment. *Geochim. Cosmochim. Acta* **57**, 3041-3061.
Yunker, M.B., Macdonald, R.W., Veltkamp, D.J., and Cretney, W.J. (1995) Terrestrial and marine biomarkers in a seasonally ice-covered Arctic estuary - integration of multivariate and biomarker approaches. *Mar. Chem*. **49**, 1-50.
Yunker, M. B., Backus, S. M., Graf Pannatier, E., Jeffries, D.S. and Macdonald, R. W. (2002) Sources and significance of alkane and PAH hydrocarbons in Canadian Arctic rivers. *Estuar. Coast. Shelf. Sci.* **55**, 1-31.
Zhang, X., Vincent, L. A., Hogg, W.D., and Niitsoo, A. (2000) Temperature and precipitation trends in Canada during the 20th century. *Atmos. Ocean* **38**, 395–

429.
Zimmermann, B. E., Porcelli, D., Frank, M., Andersson, P. S., Baskaran, M., Lee, D., and Halliday, A. N. (2009) Hafnium isotopes in Arctic Ocean water. *Geochim. Cosmochim. Acta* **73** (11), 3218-3233.

Figure 1

(a) The Mackenzie delta is the largest source of fluvial sediments to the Arctic Ocean, here illustrated with a satellite image of 15 June 1998 (http://visibleearth.nasa.org), (b) Mackenzie drainage basin (map produced by Mackenzie Basin Impact Study), (c) Mackenzie Delta sample locations with lake sediments in green, bank sediments in yellow, channel sediments in blue and suspended river sediments in red. Sampling locations are divided in upper, middle, lower and outer delta regions. The white dashed line is the driftwood line, marking the southward limit of storm surge flooding and wave action impact, (d) Mackenzie shelf sample locations collected in 1987 (Macdonald et al., 1988; Drenzek et al., 2007; Yunker et al., 1993).

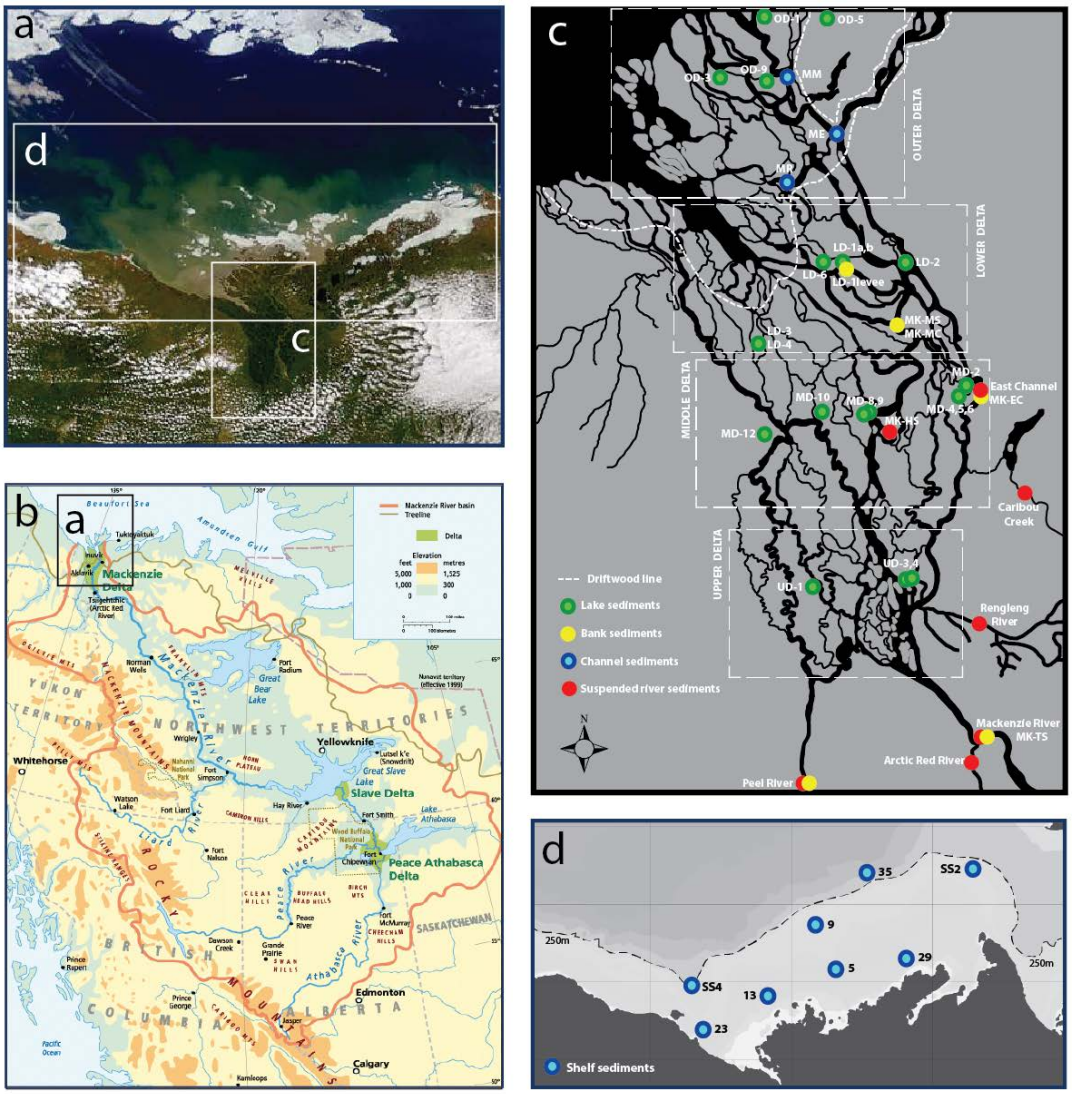

Figure 2

Particle size distributions plots of (a) bank sediments (grey) and channel sediments (black), (b) lake sediments, and (c) shelf sediments in the Mackenzie Delta and the Mackenzie shelf. Lakes LD-1a, LD-6, and the outer delta (OD) lakes are excluded from (b) as these lake sediments were size-fractionated.

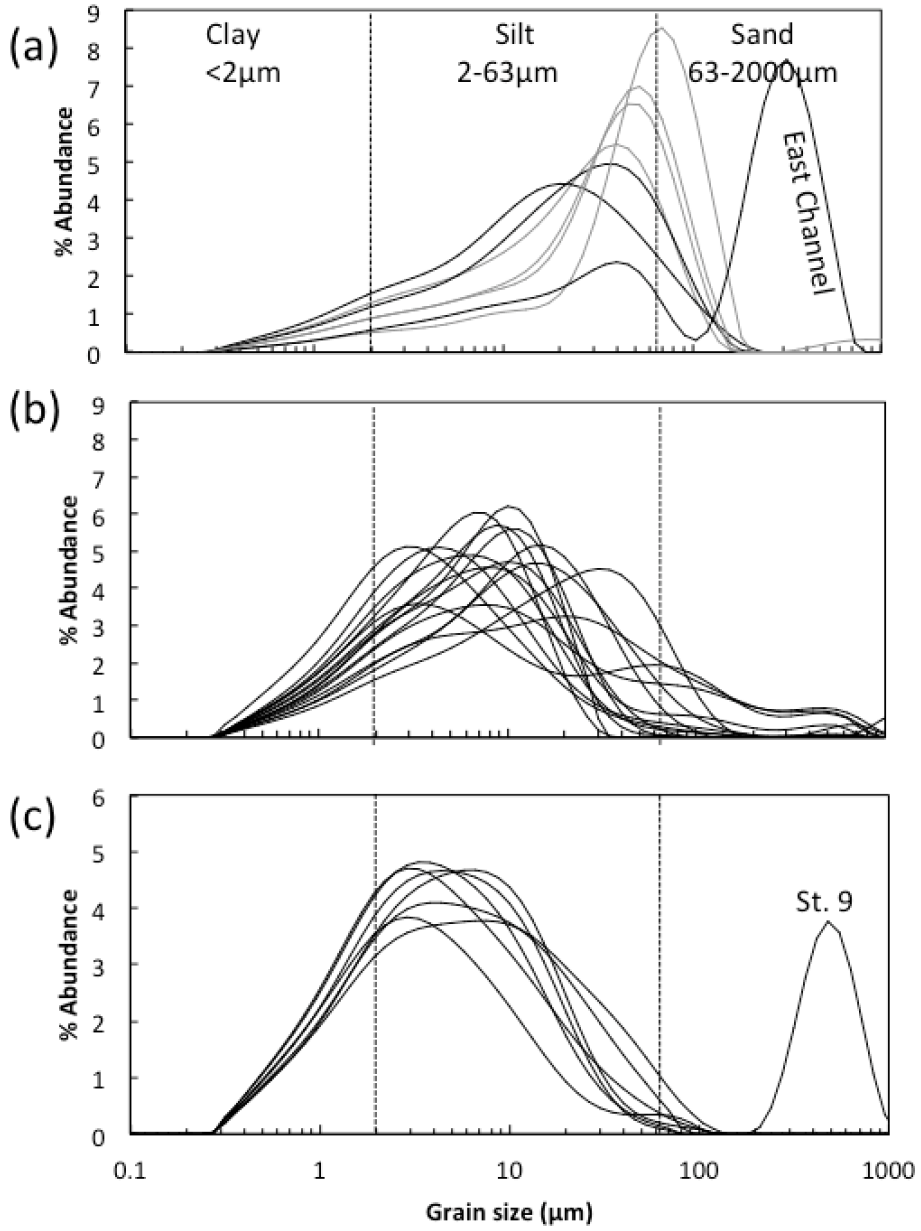

Figure 3

Across-delta patterns in mineral surface area and carbon loading, with (a) organic carbon content (%OC) against Al/Si weight ratios, (b) Al/Si weight ratios versus fraction (%) clay (<2μm), (c) mineral surface area (SA; m^2/g) against fraction clay, (d) organic carbon content (%OC) against mineral surface area with lines indicating OC:SA = 1.0 and OC:SA = 0.4 (Blair and Aller, 2012) enclosing the typical range of river suspended material and shelf sediments. Then, (e) Al/Si weight ratios versus surface area normalized organic carbon contents, expressed as OC:SA ratios (mg C/m^2), and (f) mean grain size versus OC:SA ratios. Suspended sediments in (d) and channel sediments in (c) are from Goñi et al., 2005, and shelf sediments are from this study and Goñi et al., 2005.

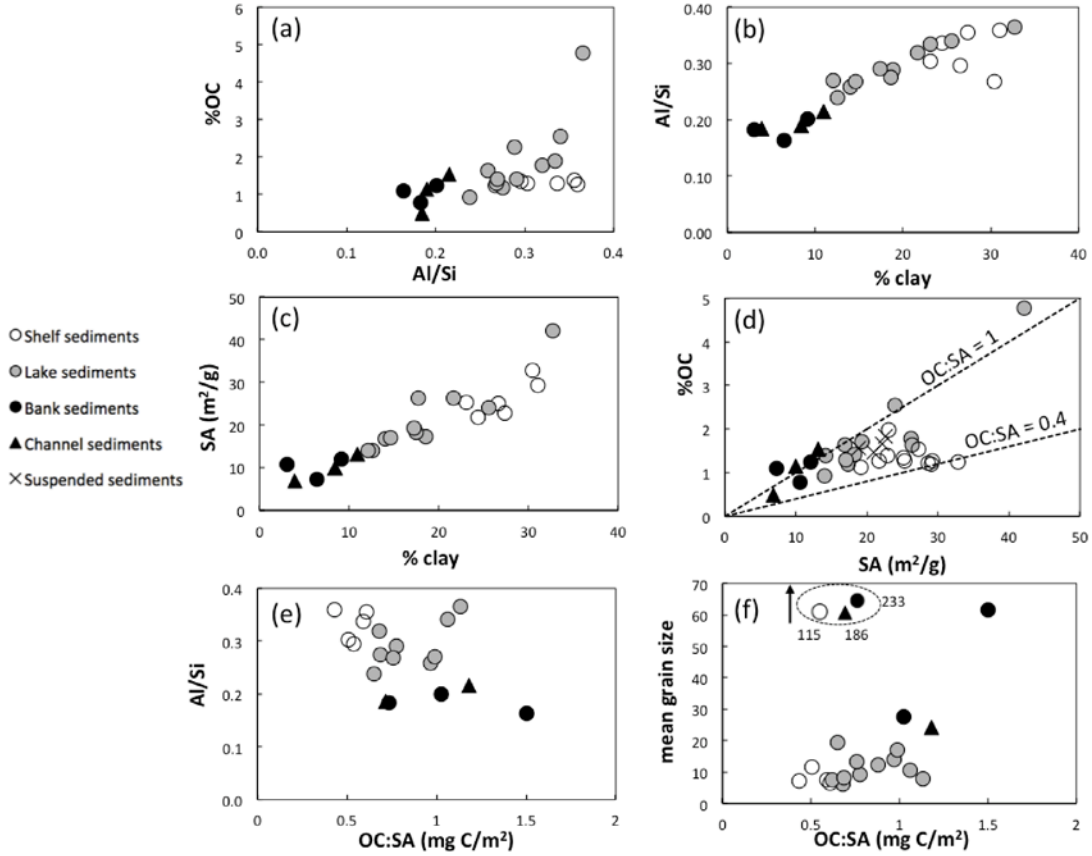

Figure 4

Concentrations of (a) %OC, (b) K, (c) Zr and (d) Rb in ppm against Al/Si weight ratios for Mackenzie delta shelf, lake and bank sediments (white, grey and black circles, respectively), Ganges-Brahmaputra suspended sediments (diamonds; Galy et al., 2008; Bouchez et al., 2011) and Amazon suspended sediments (triangles; Garçon et al., 2013; Bouchez et al., 2014).

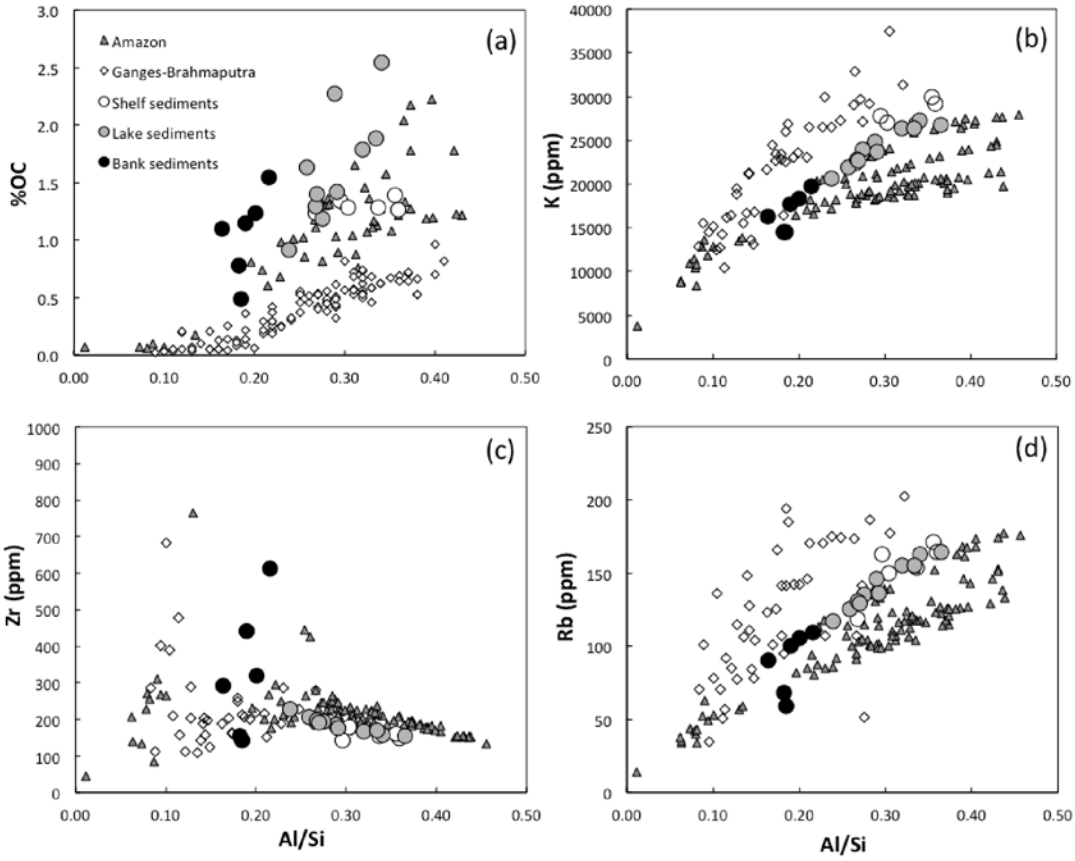

Figure 5

(a) Surface area normalized organic carbon contents (mg C/m^2), expressed as OC:SA ratios, against $\delta^{13}C$ (‰), (b) OC:SA ratios against $\Delta^{14}C$ (‰), (c) relationships between $\delta^{13}C$ and OC:SA ratios (after Blair and Aller, 2012) where the slope represents the loss of terrestrial OC ($\delta^{13}C$ of -28.5‰), and (d) relationships between $\Delta^{14}C$ and OC:SA ratios where the slope represents the loss of relatively young terrestrial OC ($\Delta^{14}C$ of -417‰), where the point marked with a (*) is excluded from the correlation. Suspended sediments are from Goñi et al., 2005, and shelf sediments are from this study and Goñi et al., 2005.

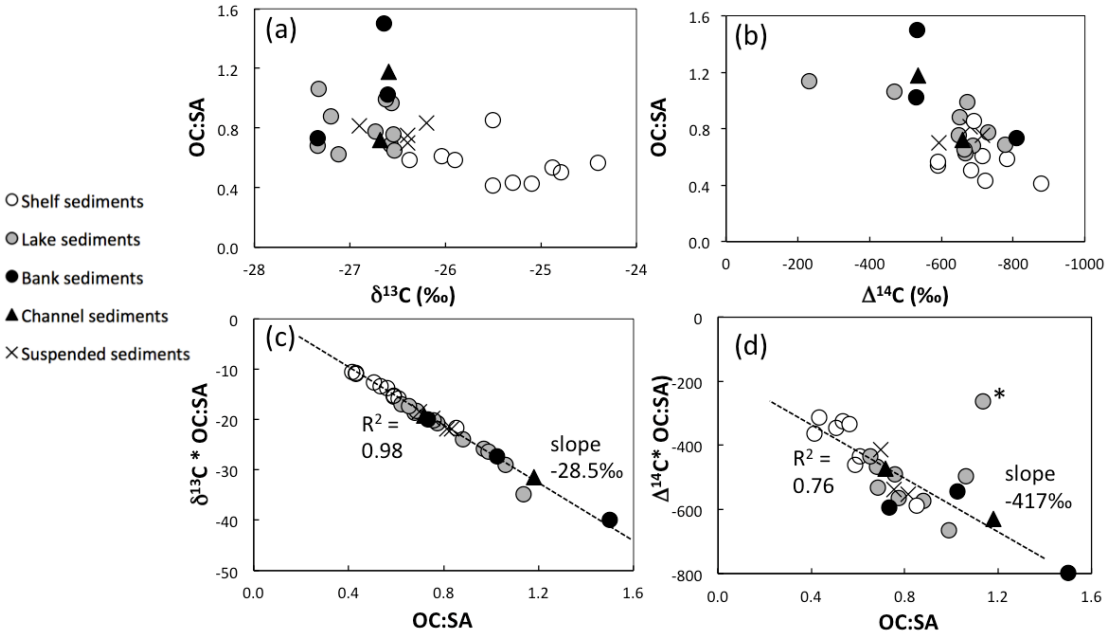

Figure 6

(a) Stable carbon (expressed as $\delta^{13}C$ in ‰) and radiocarbon (expressed as $\Delta^{14}C$ in ‰) isotopic values on bulk organic carbon. Three shelf sediments and 1987 suspended matter sediments are from Goñi et al. (2005). (b) Fraction modern (Fm) against aluminum/total OC ratio (Al/OC_{total}) □□□□□□high Al/OC ratios and low Fm correspond to petrogenic OC sources (Dellinger et al., 2014; Bouchez et al., 2014). The intercept at Fm = 0 (ca. 120000) is used for quantifying the fraction petrogenic OC and the age of biogenic OC, and (c) organic carbon content (%OC) against $\Delta^{14}C$ (‰) of biogenic OC. Bank sediments are shown as black circles, channel sediments as black triangles, lake sediments as grey circles, suspended sediments as crosses (this study and Goñi et al., 2005), and shelf sediments as open circles (this study and Goñi et al., 2005).

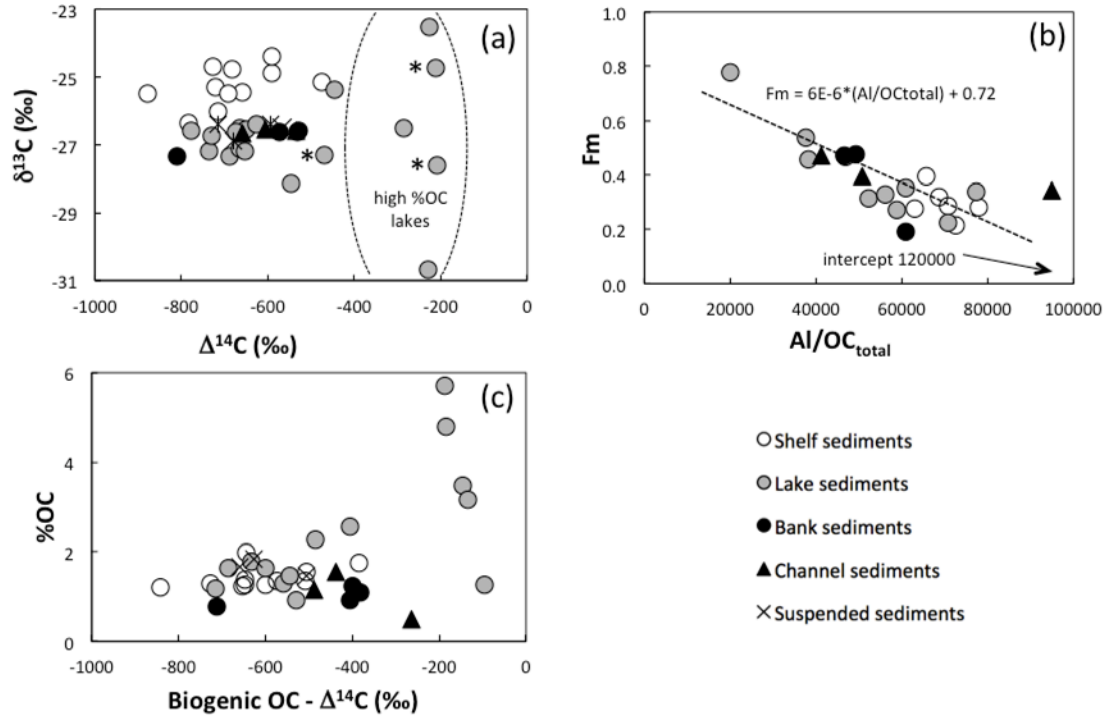

Figure 7

Neodymium isotope results (reported as ε) for (a) lake surface sediments, (b) bank sediments, and (c) channel and suspended particulate matter sediment (SPM).

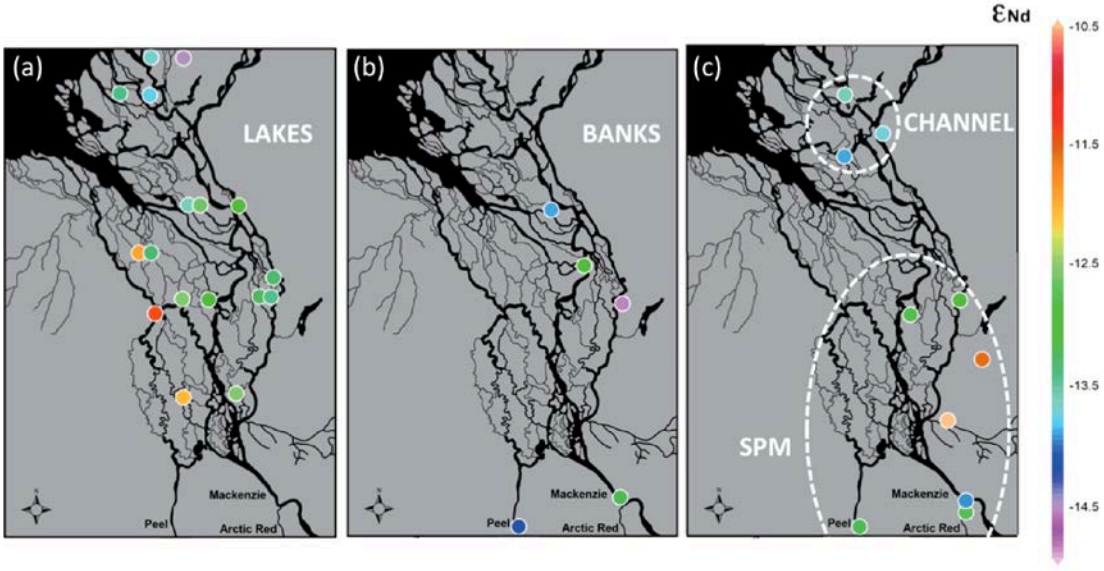

Figure 8

Variability of neodymium isotopes (expressed as ε_{Nd}) against (a) neodymium (Nd) concentration (ppm; from detrital fraction analyzed on Neptune), (c) Al/Si weight ratios, as a proxy for grain size, (d) $\Delta^{14}C$ (‰). Panel (b) shows Nd concentration (ppm; detrital fraction) against Al/Si weight ratios. Suspended and shelf sediments are from this study and Goñi et al., 2005. Note that LD-1 samples (panel d, marked with *) show similar ^{14}C values but very different εNd values (-11.2 for 2007; -13.9 for 1994).

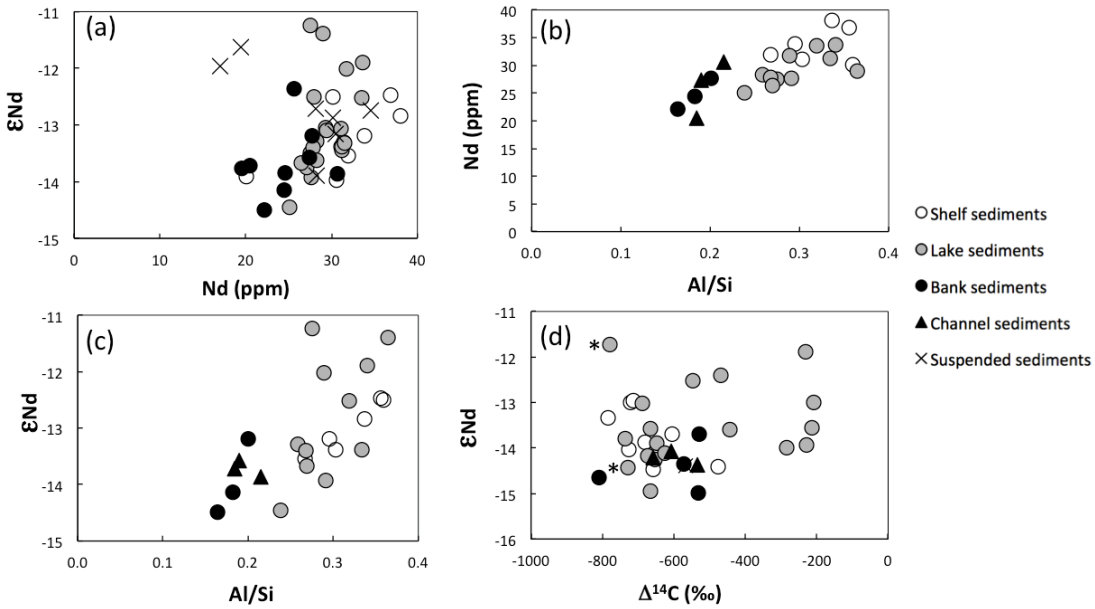

Figure 9

Deuterium isotopes (δ^2H, in ‰) of river water collected in delta lakes (crosses), and in the Mackenzie River (MK; at Tsiigehtchic; grey triangles), Peel River (white triangles), Arctic Red River (grey circles), Rengleng River (black triangles) and Caribou Creek (white squares) against Julian day. For all rivers, δ^2H generally becomes more enriched later in the sampling period, because of a gradual decrease in contribution from snow melt, but the timing and speed of this enrichment is different for each river due to factors such as latitude or elevation. The δ^2H and $\delta^{18}O$ were correlated (meteoric water line equation of $\delta^2H = 5.95 * \delta^{18}O - 55$) so the graph of $\delta^{18}O$ against Julian day was practically identical.

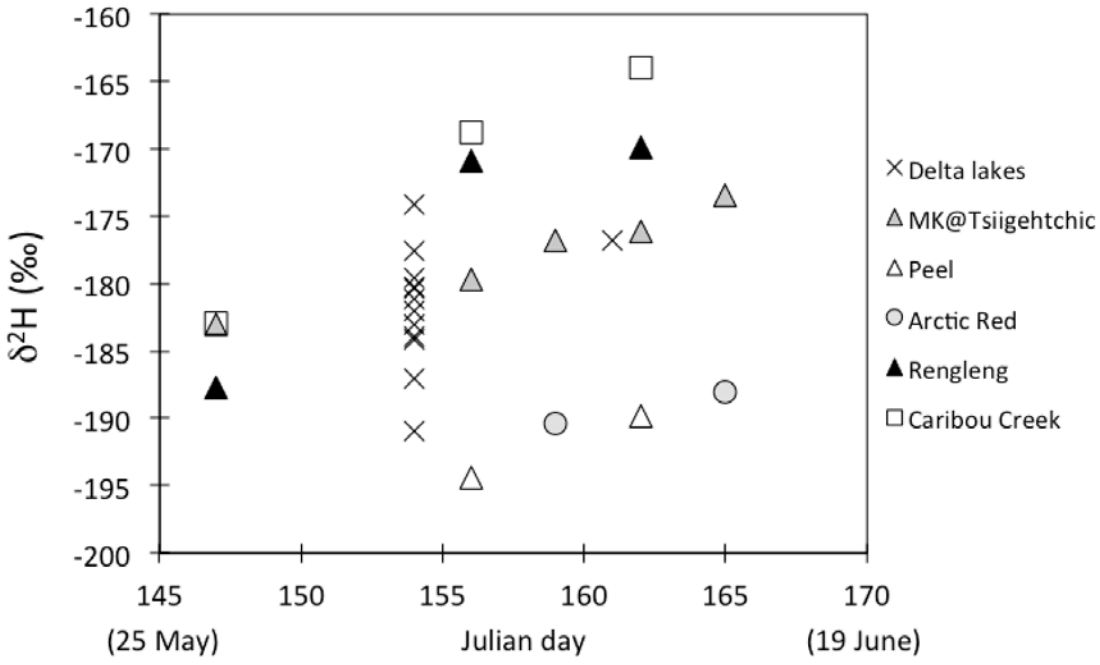

Figure 10

Close-ups of middle delta lakes to illustrate variability in sedimentation patterns. (a) Lakes MD-4 and 6 are no-closure lakes that continuously receive sediment from a small inflow channel (A) that connects through a ~5km long side branch (B) with the East Channel. MD-5 is a high-closure lake that only receives sediment through overbank flooding during peak river levels (image from Google Earth 30 June 2004), (b) MD-9 is a low-closure lake and connects during the summer months through two short channels (A, B) and another lake to a parallel branch of the Mackenzie Main channel (C), whereas MD-8 is a high-closure lake that only receives sediments during peak flow, albeit then directly from the main channel (image from Google Earth 11 June 2004). Note that the gradient in lake color is indicative for the suspended matter load; lighter grey marks a high suspended load, black a low suspended load.

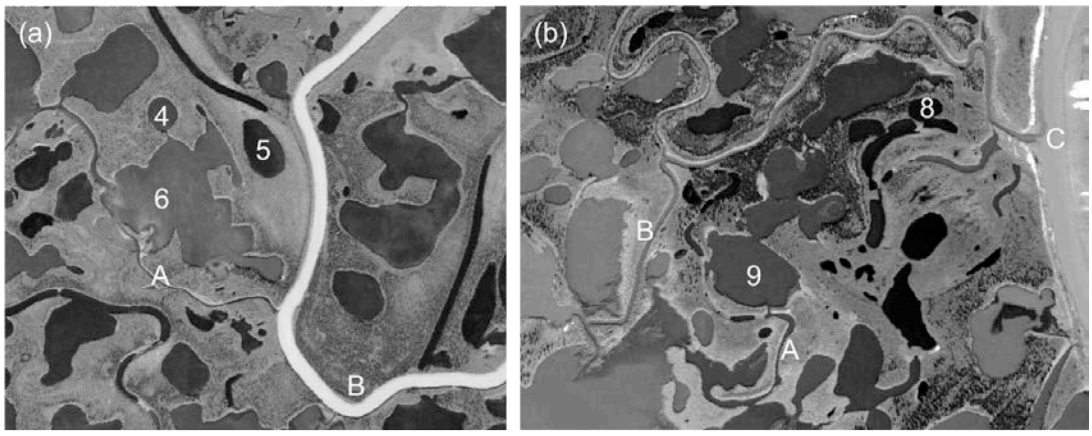

Figure 11

Degree of lake closure for the Mackenzie delta lakes, with (a) stable carbon isotopes ($\delta^{13}C$ in ‰) against $\Delta^{14}C$ of biogenic OC (in ‰, following the approach by Bouchez et al., 2014), and (b) $\Delta^{14}C$ (‰) of total OC against OC content (%). No closure lakes (black circles) are year-round connected to a river channel, low closure lakes (grey circles) are flooded during peak discharge in spring, and high closure lakes (open circles) are only flooded when water levels are exceptionally high.

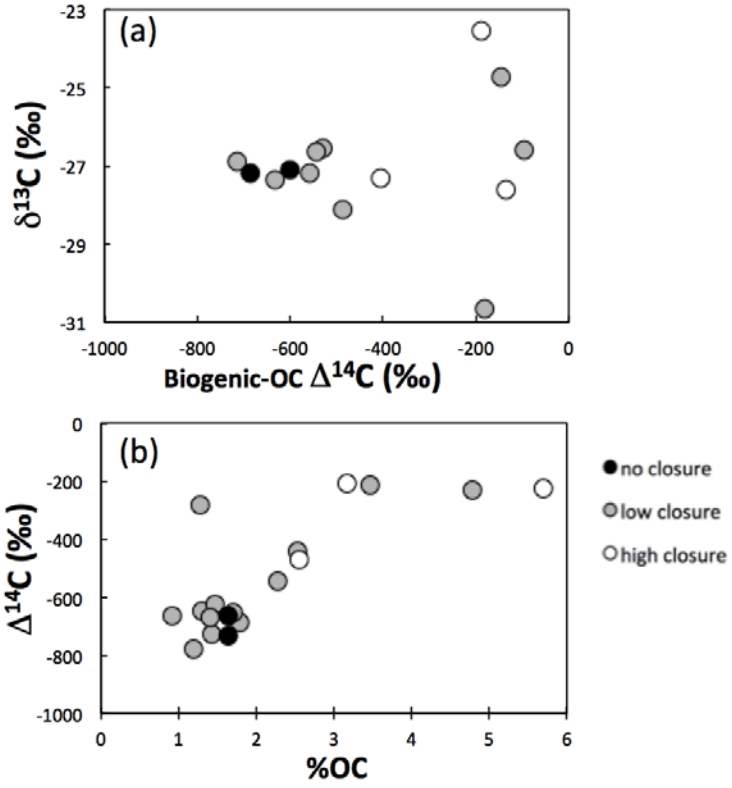

Table 1 Sampling information, location and bulk geochemical and sedimentological data. Abbreviations between brackets listed behind station/site names correspond with the abbreviations used in Figure 1. Surf. is "sampled at surface", SA is surface area, MK is Mackenzie River.

Sampling and site information							**Bulk geochemistry**				**Sedimentology**			
Station/site	Further info	Year	Date/ Month	Lat	Lon	Water depth	%OC	$\delta^{13}C$	$\Delta^{14}C$	AMS code	SA	Grain size		
				°N	°W	m		‰	‰	ETH#	m^2/g	%clay	%silt	%sand
Shelf sediments[1]														
23	G32	1987	August	69.387	138.133	69	1.35±0.04	-25.5±0.06	-658±11	54612.1.1	--	25	75	0.4
13	G35	1987	August	69.817	135.835	15	1.28±0.02	-26.4±0.09	-784±11	54613.1.1	22	24	75	0.4
29	G20	1987	August	70.307	130.953	17	1.75±0.14	-25.2±0.11	-476±9	54614.1.1	--	22	77	0.3
SS4	G30	1987	August	69.935	138.573	255	1.26±0.01	-25.3±0.04	-722[3]	-	29	31	68	0.6
9	G12	1987	August	70.737	134.165	61	1.35±0.02	-24.9±0.09	-591[4]	OS-21909[4]	25	27	49	24
35	G16	1987	August	71.408	132.333	460	1.23±0.02	-24.7±0.12	-727[3]	-	33	30	69	0.1
5	G7	1987	August	70.170	133.433	25	1.39±0.03	-26.0±0.05	-691[4]	OS-15644[4]	23	27	73	0.0
SS2	G28	1987	August	71.462	128.563	167	1.28±0.03	-24.8±0.11	-682[3]	-	25	23	75	1.7
Channel sediments[2]														
East Channel (ME)	GS-1-1	1987	July	69.007	134.633	1	0.49±0.05	-26.7±0.18	-659±11	54615.1.1	6.9	3.9	36	60
Middle Channel (MM)	GS-2-3	1987	June	69.170	135.027	1	1.14±0.03	-26.5±0.07	-606±11	54616.1.1	9.9	8.4	80	11
Reindeer Channel (MR)	GS-3-2	1987	July	68.890	135.030	1	1.54±0.06	-26.6±0.11	-534±11	54617.1.1	13	11	80	9.0
Bank sediments														
MK-East Channel (MK-EC)		2011	31-May	68.338	133.767	surf.	1.10±0.05	-26.6±0.09	-532±12	54639.1.2	7.3	6.4	74	20
MK-Tsiigehtchic (MK-TS)		2011	8-Jun	67.457	133.848	surf.	1.24±0.02	-26.6±0.11	-529±12	54638.1.1	12	9.1	81	10
Peel River		2011	5-Jun	67.338	134.873	surf.	0.78±0.04	-27.3±0.18	-810±10	54637.1.1	11	3.1	20	77
MK-main channel (MK-MS)	sand	2009	March	68.458	134.181	surf.	0.47±0.04	-26.9±0.14	--	-	--	6.4	74	20
MK-main channel (MK-MC)	clay	2009	March	68.458	134.181	surf.	1.13±0.06	-26.4±0.28	--	-	--	3.8	59	38
LD-1 levee		1994	July	68.670	134.488	surf.	0.93±0.06	-26.6±0.02	-573±11	54636.1.1	--	9.2	83	8.0
Lake sediments[5]														
OD-1	LC	1994	March	69.366	135.211	2.8	1.40±0.03	-26.6±0.12	-673±5	54635.1.1	14	12	85	2.8
OD-3	LC	1994	March	69.153	135.494	2.2	1.29±0.09	-26.5±0.19	-649±11	54632.1.1	17	15	85	0.7
OD-5	LC	1994	March	69.361	134.820	4.0	0.92±0.17	-26.5±0.06	-665±11	54631.1.1	14	13	85	2.8
OD-9	LC	1994	March	69.154	135.183	n.m.	1.70±0.02	-27.2	-652±5	54633.1.1	19	17	82	0.8

LD-1a	LC	1994	March	68.672	134.566	2.4	1.42±0.05	-26.7±0.07	-730±5	54630.1.1	18	17	82	0.5
LD-1b	LC	2007	March	68.672	134.566	2.4	1.19±0.04	-26.6±0.05	-779±11	54595.1.1	17	19	81	0.1
LD-2	LC	2009	March	68.711	134.246	2.0	3.46±0.15	-24.7±0.26	-213±11	54621.1.1	--	16	67	17
LD-3	LC	2009	March	68.481	135.221	2.6	1.54±0.01	-26.9±0.07	--	-	--	20	80	0.1
LD-4	HC	2009	March	68.490	135.261	1.2	2.55±0.07	-27.3±0.22	-468±11	54624.1.1	24	26	72	2.3
LD-6	LC	1994	March	68.673	134.696	1.7	1.47±0.03	-26.4±0.03	-626±11	54634.1.1	--	18	81	0.3
MD-2	NC	2009	March	68.358	133.767	2.2	1.63±0.09	-27.2±0.10	-735±5	54618.1.1	--	20	79	0.4
MD-4	NC	2009	March	68.321	133.863	1.3	1.88±0.01	-27.2±0.04	--	-	--	23	76	0.8
MD-5	HC	2009	March	68.320	133.848	1.4	5.70±0.18	-23.5±0.36	-228±11	54619.1.1	--	22	62	17
MD-6	NC	2009	March	68.317	133.861	1.2	1.64±0.12	-27.1±0.01	-666±11	54628.1.1	26	18	82	0.0
MD-8	HC	2009	March	68.274	134.464	3.6	3.16±0.16	-27.6±0.13	-208±5	54623.1.1	--	11	82	7.5
MD-9	LC	2009	March	68.267	134.480	1.8	1.28±0.04	-26.5±0.04	-285±5	54629.1.1	--	16	82	1.9
MD-10	LC	2009	March	68.292	134.793	2.5	1.78±0.06	-27.3±0.08	-687±11	54620.1.1	26	22	78	0.0
MD-12	LC	2009	March	68.228	135.146	2.7	4.78±0.10	-30.7±0.10	-230±12	54622.1.1	42	33	66	1.3
UD-1	LC	2009	March	67.853	134.796	4.6	2.28±0.09	-28.1±0.16	-546±12	54625.1.1	--	19	77	4.0
UD-3	LC	2009	March	67.876	134.160	1.6	2.53±0.15	-25.4±0.04	-444±5	54626.1.1	--	12	83	4.3
UD-4	LC	2009	March	67.875	134.175	2.2	1.63±0.05	-26.6±0.05	--	-	17	14	85	1.2
Suspended sediments														
Rengleng River		2011	27-May	67.756	133.862	surf.								
Caribou Creek		2011	27-May	68.089	133.492	surf.								
Arctic Red River		2011	8-Jun	67.443	133.749	surf.								
Peel River		2011	5-Jun	67.339	134.873	surf.								
MK-East Channel (MK-EC)	Inuvik	2011	28-May	68.338	133.701	surf.								
MK-Horse shoe (MK-HS)	main stem	2011	3-Jun	68.243	134.298	surf.								
MK-Tsiigehtchic (MK-TS)	main stem	2011	8-Jun	67.468	133.685	surf.			-567±6	48915.1.1				

1 Sampling information from Macdonald et al., 1988

2 Sampling information from Goñi et al., 2005

3 Data from Drenzek et al., 2007; no uncertainties or AMS analysis numbers reported.

4 Data from Goñi et al., 2005 and Drenzek et al., 2007; no uncertainties reported on $\Delta^{14}C$ ratios, AMS analysis codes (OS-) from NOSAMS.

5 Where OD is “Outer Delta”, LD is “Lower Delta”, MD is “Middle Delta” and UP is “Upper Delta”, see also Figure 1c, and "HC", LC" and "NC" is "high-closure", "low-closure" and "no closure", respectively. Lake sediments that were sampled in 1994 (Graf-Pannatier, 1998) were size-fractionated, so only the fraction < 63µm was analyzed.

Table 2

Data used to calculate burial efficiencies (BE) for Mackenzie shelf samples following the approach of Keil et al. (1997). Shelf stations marked with (*) are from Goñi et al., 2005.

Shelf station	$\delta^{13}C$ ‰	OC:SA[1]	F-terr[2] %	F-rsl[3] %	BE %
23	-25.5		89		
13	-26.4	0.59	94	54	51
29	-25.2		76		
SS4	-25.3	0.43	78	40	31
9	-24.9	0.54	71	49	35
35	-24.7		69		
5	-26.0	0.61	89	56	50
SS2	-24.8	0.51	70	47	33
*1/G1	-25.9	0.59	90	75	68
*5/G7	-25.5	0.85	84		
*9/G12	-24.4	0.56	67	72	48
*GRM1	-25.7	0.54	87	70	61
*10/G9	-25.1	0.43	78	55	43
*10/G10	-25.5	0.41	84	53	45
average±stdev	-25.3±0.6	0.55±0.12	82±9	67±9	55±12

1 Values in table 1

2 Fraction terrestrial (in %): is derived from equation (1): $\delta^{13}C_{shelf\ sediment}$ = F-marine x $\delta^{13}C_{marine}$ + F-terr x $\delta^{13}C_{river}$ where $\delta^{13}C_{shelf\ sediment}$ are the values measured in this study and in Goñi et al., 2005 (both in this table), F-marine is (1-(F-terr)), $\delta^{13}C_{marine}$ is -20.2‰ taken from Goñi et al. (2000), and $\delta^{13}C_{river}$ is the average value of five river suspended sediments (-26.5‰; Table 1).

3 Fraction remaining surface loading (in %): representing the relative decrease in mineral surface loading from river samples to shelf samples.

4 Burial efficiency (BE): here defined as the ratio of the amount of terrestrial OC that is buried on the shelf to what arrives at the delta head, calculated as BE = F-terr x F-rsl.

Table 3

Neodymium isotopic values (given as epsilon ε□□ average reproducibility of ±0.6 ε□□□□□□□□□) and major elements (in weight %) for Mackenzie shelf, channel, bank, lake and suspended sediments.

Station		**Major elements (weight %)**									
	ε_{Nd}	SiO_2	TiO_2	Al_2O_3	Fe_2O_3	MnO	MgO	CaO	Na_2O	K_2O	P_2O_5
Shelf sediments											
23	-14.0										
13	-12.8	61	0.8	18	6.6	0.1	3.4	4.3	2.3	3.2	0.3
29	-13.9										
SS4	-12.5	61	0.8	19	7.4	0.3	3.2	1.9	3.1	3.5	0.3
9	-13.2	67	0.7	17	6.4	0.1	2.7	1.6	1.5	3.3	0.3
35	-13.5	65	0.8	15	5.8	0.1	3.5	6.7	0.6	2.7	0.2
5	-12.5	62	0.8	19	7.3	0.3	3.2	2.2	2.0	3.6	0.3
SS2	-13.4	64	0.8	17	5.8	0.0	3.5	2.5	2.7	3.3	0.3
Channel sediments											
East Channel (ME)	-13.7	56	0.5	8.8	3.1	0.1	2.4	6.1	0.6	1.8	0.1
Middle Channel (MM)	-13.6	68	0.7	11	4.6	0.1	4.1	8.6	0.7	2.1	0.2
Reindeer Channel (MR)	-13.9	66	0.8	12	5.2	0.1	4.3	8.6	0.6	2.4	0.2
Bank sediments											
MK-East Channel (MK-EC)	-14.5	70	0.6	9.7	4.0	0.1	4.4	8.9	0.7	2.0	0.2
MK-Tsiigehtchic (MK-TS)	-13.2	68	0.7	12	4.8	0.1	4.2	8.3	0.6	2.2	0.2
Peel River	-14.1	58	0.5	9.0	5.0	0.1	1.7	2.4	0.5	1.8	0.3
MK-main channel (MK-MS)	-13.8										
MK-main channel (MK-MC)	-12.4										
LD-1 levee	-13.8										
Lake sediments[1]											
OD-1	-13.7	65	0.8	15	6.0	0.1	3.6	6.5	0.6	2.7	0.2
OD-3	-13.4	65	0.8	15	6.0	0.1	3.6	6.1	0.6	2.8	0.2
OD-5	-14.5	66	0.8	13	5.4	0.1	3.7	7.1	0.6	2.5	0.2

OD-9	-13.8										
LD-1a	-13.9	63	0.8	16	6.1	0.1	3.5	6.8	0.5	2.9	0.2
LD-1b	-11.2	68	0.8	16	6.0	0.1	3.7	6.8	0.6	2.9	0.2
LD-2	-13.0										
LD-3	-13.3										
LD-4	-11.9	63	0.8	18	7.2	0.1	2.7	4.3	0.4	3.3	0.3
LD-6	-13.6										
MD-2	-13.3										
MD-4	-13.4	63	0.8	18	7.5	0.1	3.1	4.2	0.5	3.2	0.3
MD-5	-13.4										
MD-6	-13.1										
MD-8	-12.5										
MD-9	-13.5										
MD-10	-12.5	65	0.9	18	7.3	0.1	2.8	2.4	0.5	3.2	0.3
MD-12	-11.4	58	0.8	18	16	0.2	2.0	1.2	0.3	3.2	0.5
UD-1	-12.0	67	0.9	16	7.0	0.1	2.6	2.1	0.5	3.0	0.3
UD-3	-13.1										
UD-4	-13.3	66	0.8	14	5.9	0.1	3.5	6.3	0.6	2.6	0.2
Suspended sediments											
Rengleng River	-12.0										
Caribou Creek	-11.6										
Arctic Red River	-12.7										
Peel River	-13.2										
MK-East Channel (MK-EC)	-12.9										
MK-Horse shoe (MK-HS)	-12.7										
MK-Tsiigehtchic (MK-TS)	-13.9										

1 Lake sediments sampled in 1994 (*in italic*; Graf-Pannatier, 1998) were size-fractionated, so only the fraction < 63µm was analyzed.

Table 4

Trace elements (ppm) for Mackenzie shelf, channel, bank, lake and suspended sediments.

Station/site	**Trace elements (ppm)**																				
	Rb	Ba	Sr	Nb	Zr	Hf	Y	Ga	Zn	Cu	Ni	Co	Cr	V	Sc	La	Ce	Nd[1]	Nd[2]	Pb	Th	U
Shelf sediments																						
13	154	1088	176	16	153	13	25	71	48	14	60	16	116	232	18	44	82	34	38	112	12	2
SS4	164	1095	179	17	150	18	26	94	41	16	66	18	141	258	16	38	92	37	30	135	14	0
9	163	1046	153	14	144	23	19	68	131	29	48	14	111	251	17	38	68	29	34	146	13	3
35	118	1094	187	15	197	2	30	19	147	37	56	18	96	181	13	43	55	27	32	17	11	4
5	171	1084	173	16	160	13	29	54	89	33	71	22	141	266	21	34	83	34	37	88	13	1
SS2	150	958	157	16	180	19	22	73	37	22	42	14	108	250	16	40	85	35	31	124	11	4
Channel sediments																						
East Channel (ME)	59	774	138	8	141	3	19	7	69	40	27	9	67	102	8	20	27	17	20	7	8	2
Middle Channel (MM)	100	1201	183	13	442	42	29	65	121	31	65	11	90	140	14	19	55	26	27	125	9	2
Reindeer Channel (MR)	110	1274	184	14	613	49	35	63	137	32	52	15	94	157	12	28	76	32	31	126	13	1
Bank sediments																						
MK-East Channel (MK-EC)	90	1016	169	12	292	29	22	71	120	27	40	13	68	119	10	21	40	21	22	136	11	0
MK-Tsiigehtchic (MK-TS)	106	1085	178	13	320	31	26	72	139	27	45	13	80	144	13	25	57	26	28	138	13	0
Peel	68	1221	92	10	155	3	26	8	137	47	42	17	89	200	10	16	36	20	24	7	10	4
Lake sediments																						
OD-1	129	1093	188	14	191	16	30	49	169	38	59	16	104	187	16	32	68	30	26	105	9	0
OD-3	130	1142	185	16	196	7	27	47	153	35	74	15	107	187	18	30	66	29	28	88	12	2
OD-5	117	1085	184	15	226	9	28	44	138	31	58	13	97	168	12	26	55	26	25	85	11	4
LD-1a	136	1136	199	15	176	7	29	55	167	35	58	17	103	195	15	24	63	28	28	110	15	1
LD-1b	135	1146	188	19	195	14	24	54	158	37	59	16	101	190	16	31	72	31	27	108	14	6
LD-4	162	1396	178	16	156	6	29	53	181	45	66	18	130	277	16	36	91	37	34	97	12	2
MD-4	155	1133	178	16	169	20	26	60	172	40	68	19	114	216	16	37	82	34	31	120	9	6
MD-10	155	1297	149	15	167	12	30	53	179	38	71	17	121	248	20	36	92	37	33	106	12	1
MD-12	164	1116	131	15	155	8	30	61	202	49	73	21	142	306	19	40	97	39	29	120	14	7
UD-1	146	1227	132	15	184	6	30	50	174	42	60	21	123	253	16	40	80	34	32	92	12	0
UD-4	125	1006	169	15	206	8	26	46	148	40	52	15	93	169	13	27	60	27	28	88	8	2

1 on combusted fraction, analyzed on XRF spectrometer at ETH-Zürich, see methods.

2 on detrital fraction measured on MS-ICP-MS Neptune at the Woods Hole Oceanographic Institution, see methods.

Table 5

Published Nd isotopic values in Arctic rivers, shelves and ocean.

Location	Sampling date[1]	εNd	Sample size (n=..)	Matrix[2]	Reference
			Shelves and ocean basins		
Canada Basin	Aug-00	-8.47	14	Entire water column; filtered waters	Porcelli et al., 2009
Amundsen Basin	Jul-01	-10.9	16	Entire water column; filtered waters	Porcelli et al., 2009
Makarov Basin	Jul-01	-10.8	8	Entire water column; filtered waters	Porcelli et al., 2009
Beaufort Shelf	Aug-10	-7.22	1	Shelf sediment	Schreiner et al., 2013
Chukchi Sea	-	-9.31	7	Sediment	Asahara et al., 2012
Bering Sea	-	-6.07	14	Sediment	Asahara et al., 2012
Northern Baltic Sea	May-90	-19.7	3	Filtered water	Andersson et al., 1992
			Estuaries		
Mackenzie	-	-14.2	2	Estuarine sediments	Asahara et al., 2012
Colville	Aug-10	-10	6	Lagoon sediments	Schreiner et al., 2013
Yukon	-	-8.3	1	Estuarine sediments	Asahara et al., 2012
Anadyr	-	-4.7	1	Estuarine sediments	Andersson et al., 2003
Kolyma	-	-12	1	Estuarine sediments	Andersson et al., 2003
Indigirka	Sep-00	-12	1	Estuarine sediments	Guo et al., 2004
Lena	Sep-00	-12	1	Estuarine sediments	Guo et al., 2004
Khatanga	Sep-00	-12	1	Estuarine sediments	Guo et al., 2004
Yenisey	Sep-00	-7.2	1	Estuarine sediments	Guo et al., 2004
Ob	Sep-00	-7.2	1	Estuarine sediments	Guo et al., 2004
			River water		
Mackenzie	-	-12.9	1	Filtered water	Zimmermann et al., 2009
Mackenzie	-	-14.3	1	River SPM	Goldstein et al., 1984
Colville	-	-5.4	2	River SPM	Schreiner et al., 2013: this study
Yukon	-	-9.44	1	River SPM	this study
Yukon	-	-9	2	Bedload and SPM	Van Laningham et al., 2009
Tanana	-	-10.7	1	Bedload	Van Laningham et al., 2009
Kolyma	6-Sep-04	-6	1	Filtered water	Porcelli et al., 2009
Lena	24-Aug-04	-13.6	1	Filtered water	Porcelli et al., 2009
Lena	-	-14.2	1	Filtered water	Zimmermann et al., 2009

Yenisey	-	-5.2	1	Filtered water	Zimmermann et al., 2009
Ob	-	-6.1	1	Filtered water	Zimmermann et al., 2009
West Greenland rivers	-	-41.5	3	River SPM	Goldstein et al., 1988
Kalix	Oct-91 to June-92	-26	5	Filtered water	Andersson et al., 2001

1 For "-" no data were provided.

2 SPM is suspended particulate matter.